AD-A112 449 STEVENS INST OF TECH .HOBOKEN NJ DAVIDSON LAB F/G 20/4
COUNTERROTATING PROPULSIVE SYSTEM.(U)
DEC 81 S TASKONAS, W R JACOBS, P LIAO N00014-77-C-0298
UNCLASSIFIED SIT-DL-81-9-2234 NL

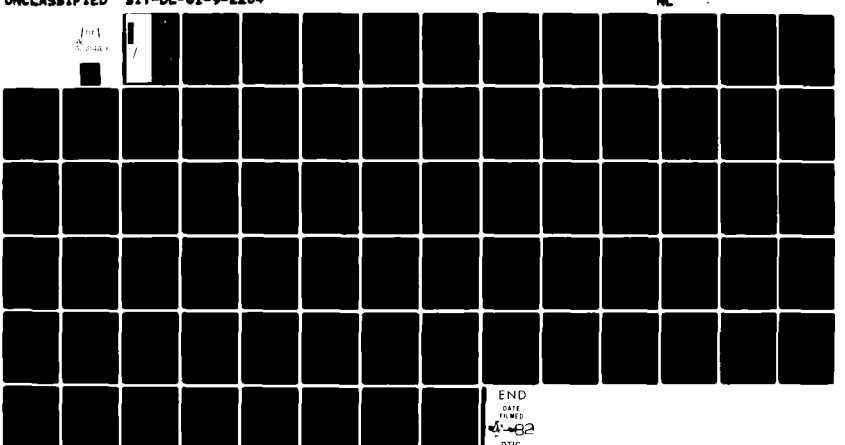

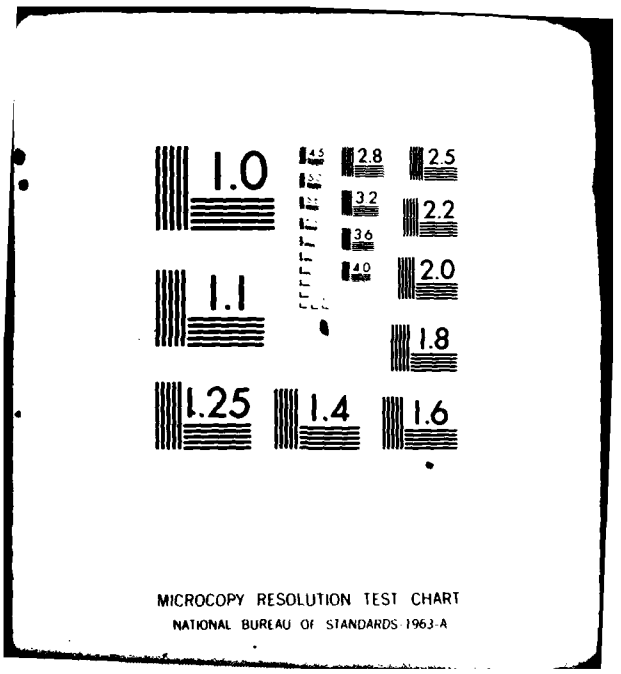
1.0
2.8
2.5
3.2
2.2
3.6
4.0
2.0
1.1
1.8
1.25
1.4
1.6
MICROCOPY RESOLUTION TEST CHART
NATIONAL BUREAU OF STANDARDS 1963-A

(12)

R-2234

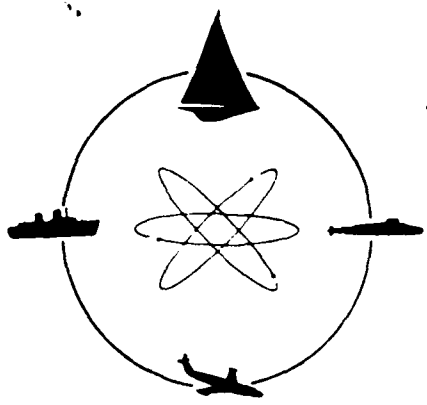

DAVIDSON LABORATORY

Report SIT-DL-81-9-2234

December 1981

COUNTERROTATING PROPULSIVE SYSTEM

by

S. TSAKONAS

W.R. JACOBS

P. LIAO

This study was sponsored by the

Naval Sea Systems Command
General Hydromechanics Research Program
Under Contract N00014-77-C-0298
Administered by The David W. Taylor
Naval Ship Research and Development Center
(DL Projects 024/4513 and 081/4804)

R-2234

STEVENS INSTITUTE
OF TECHNOLOGY

CASTLE POINT STATION
HOBOKEN, NEW JERSEY 07030

UNCLASSIFIED

SECURITY CLASSIFICATION OF THIS PAGE (When Data Entered)

REPORT DOCUMENTATION PAGE		READ INSTRUCTIONS BEFORE COMPLETING FORM
1. REPORT NUMBER SIT-DL-81-9-2234	2. GOVT ACCESSION NO. AD-A112 449	3. RECIPIENT'S CATALOG NUMBER
4. TITLE (and Subtitle) COUNTERROTATING PROPULSIVE SYSTEM.		5. TYPE OF REPORT & PERIOD COVERED FINAL 6. PERFORMING ORG. REPORT NUMBER
7. AUTHOR(s) S. Taskonas, W.R. Jacobs, and P. Liao.		8. CONTRACT OR GRANT NUMBER(s) N00014-77-C-0298
9. PERFORMING ORGANIZATION NAME AND ADDRESS Davidson Laboratory STEVENS INSTITUTE OF TECHNOLOGY 711 Hudson Street, Hoboken, NJ 07030		10. PROGRAM ELEMENT, PROJECT, TASK AREA & WORK UNIT NUMBERS 61153N R02301 SR 023 01 01
11. CONTROLLING OFFICE NAME AND ADDRESS DAVID W. TAYLOR NAVAL SHIP RESEARCH AND DEVELOPMENT CENTER, Code 1505 Bethesda, MD 20084		12. REPORT DATE December 1981 13. NUMBER OF PAGES x + 66 pp.
14. MONITORING AGENCY NAME & ADDRESS(if different from Controlling Office) OFFICE OF NAVAL RESEARCH 800 N. Quincy Street Arlington, VA 22217		15. SECURITY CLASS. (of this report) Unclassified. 15a. DECLASSIFICATION/DOWNGRADING SCHEDULE

16. DISTRIBUTION STATEMENT (of this Report)

APPROVED FOR PUBLIC RELEASE; DISTRIBUTION UNLIMITED.

17. DISTRIBUTION STATEMENT (of the abstract entered in Block 20, if different from Report)

18. SUPPLEMENTARY NOTES

Sponsored by the Naval Sea Systems Command General Hydromechanics Research Program administered by the David W. Taylor Naval Ship Research and Development Center, Code 1505, Bethesda, MD 20084.

19. KEY WORDS (Continue on reverse side if necessary and identify by block number)

Hydrodynamics

Counterrotating Propulsive Systems

20. ABSTRACT (Continue on reverse side if necessary and identify by block number)

Linearized unsteady lifting surface theory has been applied in the study of counterrotating propeller systems with equal or unequal number of blades operating in uniform or nonuniform inflow fields when both units are rotating with the same RPM. The mathematical model takes into account as realistically as possible the geometry of the propulsive device, the mutual interaction of both units and the three-dimensional —

[Cont'd]

DD FORM 1 JAN 73 1473 EDITION OF 1 NOV 65 IS OBSOLETE
S/N 0102-014-6601

UNCLASSIFIED

SECURITY CLASSIFICATION OF THIS PAGE (When Data Entered)

20. Abstract (Cont'd)

spatially varying inflow field. The propeller blades lie on a helicoidal surface of varying pitch, have finite thickness and arbitrary planform, camber and sweep angle. The inflow field of the after propeller is modified by taking into account the effect of the race of the forward propeller, so that potential and viscous effects of the forward propeller are incorporated. These additional effects play an important role in determining the unsteady loading of the after propeller. This, together with some refinements introduced in the numerical procedure, has brought the theoretical results into better agreement with experiments. A computer program has been developed adaptable to a high-speed digital computer (CDC 6600-7600, Cyber 176) for counter-rotating systems of equal and unequal number of blades, in uniform flow for comparison with existing experiments.

STEVENS INSTITUTE OF TECHNOLOGY
DAVIDSON LABORATORY
CASTLE POINT STATION
HOBOKEN, NEW JERSEY

Report SIT-DL-81-9-2234

December 1981

COUNTERROTATING PROPULSIVE SYSTEM

by

S. Tsakonas, W.R. Jacobs, and P. Liao

This study was sponsored by the
Naval Sea Systems Command
General Hydromechanics Research Program
Under Contract N00014-77-C-0298
Administered by The David W. Taylor
Naval Ship Research and Development Center
(DL Projects 024/4513 and 081/4804)

Approved:

John P. Breslin

John P. Breslin
Director

ABSTRACT

Linearized unsteady lifting surface theory has been applied in the study of counterrotating propeller systems with equal or unequal number of blades operating in uniform or nonuniform inflow fields when both units are rotating with the same RPM. The mathematical model takes into account as realistically as possible the geometry of the propulsive device, the mutual interaction of both units and the three-dimensional spatially varying inflow field. The propeller blades lie on a helicoidal surface of varying pitch, have finite thickness and arbitrary planform, camber and sweep angle. The inflow field of the after propeller is modified by taking into account the effect of the race of the forward propeller, so that potential and viscous effects of the forward propeller are incorporated. These additional effects play an important role in determining the unsteady loading of the after propeller. This, together with some refinements introduced in the numerical procedure, has brought the theoretical results into better agreement with experiments. A computer program has been developed adaptable to a high-speed digital computer (CDC 6600-7600, Cyber 176) for counterrotating systems of equal and unequal number of blades, in uniform flow for comparison with existing experiments.

ACKNOWLEDGMENT

The authors are indebted to Drs. J.P. Breslin and T.R. Goodman for the specific modifications to the downstream induced velocity in the race of a propeller, and to Dr. Breslin for the particular procedure to account for the effect of the viscous wake of the forward propeller on the after propeller.

KEYWORDS

Hydrodynamics
Counterrotating Propulsive Systems

TABLE OF CONTENTS

NOMENCLATURE

A	subscript index of after propeller
a	$\Omega r_o/U$
F	subscript index of forward propeller
$F_{x,y,z}$	forces in axial, horizontal and vertical directions
$I^{(\bar{m})}(x)$	defined in Equation (7a)
$I_m(\nu)$	modified Bessel function of order m
i	subscript index of control point
j	subscript index of loading point
$K_m(\nu)$	modified Bessel function of order m
K_{ji}	kernel function of integral equation
$\bar{K}_{ji}, \bar{K}'_{ji}$	modified kernels, after chordwise-integrations
L(r)	spanwise loading distribution, lb/ft
$L^{(\bar{n})}(\rho)$	spanwise loading components (coefficients of chordwise distribution), lb/ft
ℓ_k	integer multiple
$\bar{m}$	order of lift operator
m_k	index of summation
N_F, N_A	number of blades of forward and after propellers
$\bar{n}$	order of chordwise mode
n	blade index
P	perturbation pressure
$Q_{x,y,z}$	moments about x-, y- and z-axes
q_i	order of blade harmonic
r	radial coordinate of control point
r	superscript index of control point
r_{Ao}	after propeller radius
r_{Fo}	forward propeller radius
S_j	lifting surface
t	time
U	uniform velocity
u	variable of integration

$V_j(r)$	Fourier coefficients of velocity normal to the blade
$W_j(x,r,\varphi;t)$	induced velocity at control point
x,x'	longitudinal coordinate of control point
$x(x'),r,\varphi$	cylindrical coordinate system of control points
y	horizontal Cartesian coordinate
z	vertical Cartesian coordinate
β	hydrodynamic pitch angle
ϵ	distance between the two propeller planes
$\Theta(\bar{n})$	chordwise mode
θ_j	angular coordinate of loading point
θ_α	angular chordwise location of loading point
θ_{bF},θ_{bA}	projected semichord length, in radians, of forward and after propellers
$\bar{\theta}_{jn}$	$\frac{2\pi}{N_j}(n-1)$, $n=1, \ldots N_j$
$\theta_p(r)$	geometric pitch angle
$\Lambda^{(\bar{n})}(x)$	defined in Equation (7b)
λ_k	positive integer multiple
ξ,ξ'	longitudinal coordinate of loading point
$\xi(\xi'),\rho,\theta$	cylindrical coordinate system of loading points
ρ	radial coordinate of loading point
ρ	superscript index of loading point
ρ_f	mass density of fluid
σ	angular measure of skewness
$\$(\bar{m})$	generalized lift operator
φ_i	angular coordinate of control point
φ_α	angular chordwise location of control point
Ω	angular velocity of propeller (absolute value)

INTRODUCTION

The combination of two counterrotating propellers on fast ships has been shown to offer considerable improvement in propulsive efficiency when compared with a single screw [1].* Furthermore, since the total required power is divided between two propellers, this results in a reduction of blade loadings and hence the inception of cavitation is delayed. These are the main advantages of this propulsive system; its principal disadvantage lies in the mechanical complications in transmitting power through a coaxial counterrotating shaft.

The CR (counterrotating) propulsive system is also expected to have more favorable vibrational behavior. From tests of a 4-0-5 CR system (4-bladed forward and 5-bladed after propeller) in the wake of a model of a fast cargo liner [2], it appears that the ratios of amplitudes of excitation to mean thrust are comparable to those of a single screw providing the same power. However in these tests the nonuniform wake is by far the dominating cause of vibration. The effects of the interaction of both propellers are small in comparison and the higher frequency excitations cannot be determined at all accurately.

A better understanding of the mechanism of the interaction can be obtained by considering the CR system under open-water conditions (uniform inflow field) so that wake harmonics are not present to mask the interaction phenomenon.

The calculation procedure is based on the analysis of Reference [3] for the cases of CR systems of equal and unequal blade number, operating at equal or unequal RPM in uniform and nonuniform inflow fields. In that reference, the true geometry of the helicoidal blades was taken into account with the exception that blade thickness was assumed negligible.

In Reference [4], CR systems of equal and unequal number of blades are considered operating at equal RPM in a uniform inflow field. The blade thickness effects are also considered as additional velocity perturbations

*References in text matter refer to similarly numbered references listed at the end of this report (pp. 54-55).

on the LH (left-hand) sides of the two surface integral equations which state the kinematic conditions on both units of the CR system.

The development of this pair of surface integral equations is based on a linearized unsteady lifting surface theory as adapted to the marine propeller case. Their kernel functions are derived by means of the acceleration potential method and the surface integrals are reduced to line integrals by employing the mode approach in conjunction with the "generalized lift operator" technique [5]. Then by the collocation method the line integral equations are reduced to two simultaneous sets of algebraic equations. Finally, the solution of these is obtained by an iterative procedure, assuming at first that the effect of the after propeller on the forward propeller, except for the velocity field due to the thickness of its blades, may be neglected. The computation procedure is adapted to a high-speed digital computer (CDC-6600, 7600, or Cyber 176).

In Reference [4] calculations were performed for two CR (counterrotating) configurations for which data are available from tests at the David W. Taylor Naval Ship Research and Development Center,[6,7] with disappointing results. Re-examination of the theoretical development has indicated that two important factors have been neglected: that due to the forward propeller wake induction on the after propeller, and that due to the effect of viscosity.

In a series of systematic calculations of the velocity field around an operating propeller, it was found that at points in the race the characteristics of the velocity field were quite different from those outside the race. Since the after propeller is located in the race of the forward propeller, an analysis has been developed taking cognizance of this fact. A correction has been incorporated in the program at the point where the induced velocity on the after propeller due to the presence of the forward operating propeller is determined.

It is also recognized that since both components of the CR system are located in close proximity to each other, the "potential" approach will not be sufficient to study the interaction phenomenon; the effect of viscous wake must be taken into account. In the absence of wake measurements at the plane of the after propeller, an approximate method has been utilized by adapting the development of Reference [16] to the CR system in order to

provide the harmonic content of the viscous wake of the forward propeller.

Both of these additional factors have been incorporated in the present study.

This study is sponsored by the Naval Sea Systems Command General Hydromechanics Research Program under Contract N00014-77-C-0298, administered by the David W. Taylor Naval Ship Research and Development Center; Davidson Laboratory Projects 024/4513 and 081/4804.

LINEARIZED UNSTEADY LIFTING SURFACE THEORY

Two counterrotating propellers are operating in the flow of an ideal incompressible fluid. The propeller arrangement and the coordinate system are shown in Figure 1.

The basic relation of the interaction phenomenon is that the negative velocities induced by the propulsion system on each propeller lifting surface should be balanced by the downwash velocity distribution at that surface, thus expressing the requirement of an impermeable boundary. The kinematic boundary conditions on both lifting surfaces are expressed as two simultaneous surface integral equations, symbolically represented as

$$W_F(x_F, r_F, \varphi_F; t) = \iint_{S_F} \Delta P_F(\xi_F, \rho_F, \theta_F; t) \cdot K_{FF}(x_F, r_F, \varphi_F; \xi_F, \rho_F, \theta_F; t)\, dS_F + \iint_{S_A} \Delta P_A(\xi_A', \rho_A, \theta_A; t) \cdot K_{AF}(x_F, r_F, \varphi_F; \xi_A', \rho_A, \theta_A; t)\, dS_A \tag{1}$$

$$W_A(x_A', r_A, \varphi_A; t) = \iint_{S_F} \Delta P_F(\xi_F, \rho_F, \theta_F; t) \cdot K_{FA}(x_A', r_A, \varphi_A; \xi_F, \rho_F, \theta_F; t)\, dS_F + \iint_{S_A} \Delta P_A(\xi_A', \rho_A, \theta_A; t) \cdot K_{AA}(x_A', r_A, \varphi_A; \xi_A', \rho_A, \theta_A; t)\, dS_A \tag{2}$$

where

$x(x'), r, \varphi$ and $\xi(\xi'), \rho, \theta$: cylindrical coordinates of control and loading points, respectively

F and A: subscripts indicating forward and after propeller

t: time, sec

S_F, S_A: forward and after propeller surfaces, ft^2

W_F, W_A: velocity distributions normal to forward and after propellers, ft/sec

$\Delta P_F, \Delta P_A$: unknown loadings; pressure jumps across the lifting surfaces, lb/ft^2, i.e., $\Delta P = P_- - P_+$ pressure difference between back (suction side) and face (pressure side)

K_{ji}: kernel function representing the induced velocity on an element i of a blade due to unit amplitude load located at each and every element j, ft/lb-sec

The second term on the RH (right-hand) side of Eq.(1) and the first term on the RH side of Eq.(2) are the interaction effects. The remaining terms are the self-induced velocities by the individual propellers.

The unknown loadings and the onset velocity distributions are cyclic in nature. Then for a CR system with right-hand aft propeller and left-hand forward propeller rotating at equal RPM

$$\Delta P_F(\xi_F, \rho_F, \theta_F; t) = \mathrm{Re} \sum_{\lambda_k=0}^{\infty} \overline{\Delta P}_F^{(\lambda_k)} (\xi_F, \rho_F, \theta_F) e^{-i\lambda_k \Omega t}$$

$$\Delta P_A(\xi_A', \rho_A, \theta_A; t) = \mathrm{Re} \sum_{\lambda_k=0}^{\infty} \overline{\Delta P}_A^{(\lambda_k)} (\xi_A', \rho_A, \theta_A) e^{i\lambda_k \Omega t} \tag{3}$$

$$W_F(x_F, r_F, \varphi_F; t) = \mathrm{Re} \sum_{q_F=0}^{\infty} \overline{W}_F^{(q_F)} (x_F, r_F, \varphi_F) e^{-iq_F \Omega t}$$

$$W_A(x_A', r_A, \varphi_A; t) = \mathrm{Re} \sum_{q_A=0}^{\infty} \overline{W}_A^{(q_A)} (x_A', r_A, \varphi_A) e^{iq_A \Omega t} \tag{4}$$

where q_i designates the order of shaft frequency or order of harmonic of the inflow field, λ_k that of the loading distribution to be determined by the analysis, and Ω is the absolute value of the angular velocity of each propeller (q_i and λ_k are both positive integers). The known downwash velocities and the unknown loadings are expressed in a complex conjugate form in (3) and (4), where finally the real part is taken.

The velocities W_i are caused by flow disturbances such as those due (1) to wake, (2) to incident flow angle which is the difference between the geometric pitch angle θ_p of the propeller blade and the advance angle (hydrodynamic pitch angle) $\beta = \tan^{-1} U/\Omega r$ where U is forward speed and r is the radial location of the corresponding helix, (3) to blade camber, (4) to "non-planar" blade thickness, and (5) to the effects of the thickness of the blades of each propeller on the velocity field of the other. The wake disturbances of W_A also include the wake induction of the forward propeller on the after propeller since the latter operates in the race of the forward propeller. Within the limits of the linear theory, the effects of the flow disturbances can be obtained separately and then simply added together.

Although the analysis applies to both nonuniform and uniform inflow, as mentioned earlier, the solution by an iterative procedure will be restricted to the uniform inflow case (no wake). Furthermore, the disturbance due to the so-called "non-planar" thickness (since a propeller blade lies on a helicoidal surface of variable pitch, its thickness affects its own velocity field) will be ignored as negligibly small.[9,10]

After the chordwise integrations are performed by means of the mode approach and the generalized lift operator technique, the pair of surface integral equations (1) and (2) are reduced to the following set of line integral equations for given q_i, order of shaft frequency, given $\bar{m}$, order of lift operator, and $\bar{n}$, order of chordwise mode shapes, for the case of equal RPM:

$$\frac{\bar{W}_F^{(q_F,\bar{m})}}{U}(r_F) = \int_{\rho_F} L_F^{(q_F,\bar{n})}(\rho_F) \sum_{m_1=-\infty}^{\infty} \bar{K}_{FF}^{(\bar{m},\bar{n})}(m_1 = q_F + \ell_1 N_F)\, d\rho_F + \int_{\rho_A} \sum_{\lambda_2=0}^{\infty} \sum_{m_2=0}^{\infty} L_A^{(\lambda_2 = q_F + 2\ell_2 N_A, \bar{n})}(\rho_A) \cdot \bar{K}_{AF}^{(\bar{m},\bar{n})}(m_2 = q_F + \ell_2 N_A)\, d\rho_A \qquad (5)$$

$$\frac{\bar{W}_A^{(q_A,\bar{m})}}{U}(r_A) = \int_{\rho_F} \sum_{\lambda_3=0}^{\infty} \sum_{m_3=0}^{\infty} L_F^{(\lambda_3 = q_A + 2\ell_3 N_F, \bar{n})}(\rho_F) \cdot \bar{K}_{FA}^{(\bar{m},\bar{n})}(m_3 = q_A + \ell_3 N_F)\, d\rho_F + \int_{\rho_A} L_A^{(q_A,\bar{n})}(\rho_A) \sum_{m_4=-\infty}^{\infty} \bar{K}_{AA}^{(\bar{m},\bar{n})}(m_4 = q_A + \ell_4 N_A)\, d\rho_A \qquad (6)$$

Here $L_F^{(\bar{n})}(\rho_F)$ and $L_A^{(\bar{n})}(\rho_A)$ are the unknown normal loading components of the $\bar{n}$ chordwise mode for each blade in lb/ft of span, N_F and N_A are the blade number of forward and after propellers, and ℓ_k is integer. The bars and superscripts $\bar{m}$ and $\bar{n}$ indicate that the quantities have been integrated along the chord.

The values of λ_k and m_k shown in (5) and (6) are arrived at by equating the time-dependence on LH and RH sides so that

$e^{-iq_F\Omega t} = e^{-i\lambda_1\Omega t}$	for the first term of the first integral equation
$e^{-iq_F\Omega t} = e^{i(\lambda_2-2m_2)\Omega t}$	for the second term of that equation
$e^{iq_A\Omega t} = e^{-i(\lambda_3-2m_3)\Omega t}$	for the first term of the second integral equation
$e^{iq_A\Omega t} = e^{i\lambda_4\Omega t}$	for the second term of that equation

and from the summation over all blades of a propeller which is represented by

$$\sum_{n=1}^{N} e^{\pm i(m_k-\lambda_k)\bar{\theta}_n} = \begin{cases} N \text{ for } m_k-\lambda_k=\ell_k N, \ell_k=0,\pm 1, \ldots \\ 0 \text{ otherwise} \end{cases}$$

where $\bar{\theta}_n = 2\pi(n-1)/N$.

The respective kernels are derived in Reference [3] for RH forward propeller and LH after propeller. For LH forward and RH after propeller, they are given in the following section in final form.

THE KERNEL FUNCTIONS

The Kernels $\bar{K}_{FF}$ and $\bar{K}_{AA}$

These functions describe the self-induced velocity at a point on a propeller blade due to unit amplitude load at various locations on all the blades of the same propeller. The development for a right-hand propeller is given in Reference [10] and yields

$$\sum_{m=-\infty}^{\infty} \bar{K}^{(\bar{m},\bar{n})}_{(m=q+\ell N)} = \left\{\frac{-N}{4\pi\rho_f U^2 r_o}\right\} \frac{r\, e^{-iq\Delta\sigma}}{a\sqrt{1+a^2r^2}}$$

$$\sum_{\substack{m=-\infty \\ m=q+\ell N}}^{\infty} \left\{g(0) - \frac{i}{\pi}\int_0^{\infty} \frac{g(u)-g(-u)}{u}\, du\right\} \qquad (7)$$

where

$$g(u) = (IK)_m B'(u) e^{i\frac{u}{a}\Delta\sigma}$$

$$(IK)_m = \begin{cases} I_m(|u+a\ell N|\rho) K_m(|u+a\ell N|r) & \text{for } \rho < r \\ I_m(|u+a\ell N|r) K_m(|u+a\ell N|\rho) & \text{for } r < \rho \end{cases}$$

$$B'(u) = \left(au + a^2\ell N + \frac{m}{r^2}\right) \cdot \left(au+a^2\ell N+\frac{m}{\rho^2}\right) I^{(\bar{m})}\left((q-\frac{u}{a})\theta_b^r\right) \Lambda^{(\bar{n})}\left((q-\frac{u}{a})\theta_b^\rho\right)$$

ρ_f = fluid mass density, slugs/ft^3

r_o = propeller radius, ft

$\Delta\sigma = \sigma^r - \sigma^\rho$ = difference between skewness of the blade at the control point r and skewness at a loading point ρ, radians

$a = \Omega r_o/U$ and ρ and r are also non-dimensionalized by r_o

$\theta_b^r, \theta_b^\rho$ = subtended angle of projected semichord of blade at r, at ρ, radians

$I_m(\ )$ = modified Bessel function of first kind

$K_m(\ )$ = modified Bessel function of second kind

$\ell = 0, \pm1, \pm2, \ldots$

In this equation the chordwise integration is represented by

$$I^{(\bar{m})}(x) = \frac{1}{\pi}\int_0^{\pi} \Phi(\bar{m}) e^{ix\cos\varphi_\alpha} d\varphi_\alpha \qquad (7a)$$

where $\Phi(\bar{m})$ is the lift operator function, and

$$A^{(\bar{n})}(y) = \frac{1}{\pi}\int_0^{\pi} \Theta(\bar{n}) e^{-iy\cos\theta_\alpha} \sin\theta_\alpha d\theta_\alpha \qquad (7b)$$

where $\Theta(\bar{n})$ is the chordwise mode shape selected. (See References [3,5,9,10].)

In Eq.(6), the kernel function

$$\sum_{m_4=-\infty}^{\infty} \bar{K}_{AA}^{(\bar{m},\bar{n})} \quad (m_4 = q_A + \ell_4 N_A)$$

is given by Eq.(7) with $q=q_A$, $N=N_A$, $r=r_A$, and $\rho=\rho_A$. However, $r_o=r_{FO}$, the radius of the forward propeller.

In Eq.(5), the kernel function

$$\sum_{m_1=-\infty}^{\infty} \bar{K}_{FF}^{(\bar{m},\bar{n})} \quad (m_1 = -q_F + \ell_1 N_F)$$

is given by Eq.(7) but with $q=-q_F$, $N=N_F$, $r=r_F$, and $\rho=\rho_F$. This is equivalent to the conjugate of Eq.(7). In both Eqs.(5) and (6), the radial positions r and ρ and the inverse advance ratio a are non-dimensionalized by forward propeller radius r_{FO}.

The Kernels $\bar{K}_{AF}$ and $\bar{K}_{FA}$

These are the kernels of the cross-coupling terms of Eqs.(5) and (6). Let the distance between the propeller planes of the two units of the CR system be c (in terms of r_{FO}). Then for a RH after propeller at a distance c from a LH forward propeller operating at the same RPM, the derivations of Reference [3] can be reduced to the following final forms:

$$\bar{K}_{AF}^{(\bar{m},\bar{n})}(m_2=q_F+\ell_2 N_A\geq 0)=\left\{\frac{-N_A}{4\pi\rho_f U^2 r_{F0}}\right\}\frac{r_F}{a\sqrt{1+a^2 r_F^2}}\,e^{im_2(2\sigma_A+a\epsilon)}$$

$$\cdot\, e^{iq_F(\sigma_F-\sigma_A-a\epsilon)}\left\{A(0)B(0)-\frac{i}{\pi}\int_0^\infty[A(u)B(u)-A(-u)B(-u)]\frac{du}{u}\right\} \tag{8}$$

where

$$A(u)=\begin{cases} I_{m_2}(|u-a(m_2-q_F)|\rho_A)K_{m_2}(|u-a(m_2-q_F)|r_F) & \text{for } \rho_A\leq r_F \\ I_{m_2}(|u-a(m_2-q_F)|r_F)K_{m_2}(|u-a(m_2-q_F)|\rho_A) & \text{for } r_F<\rho_A \end{cases}$$

$$B(u)=\left[au-a^2(m_2-q_F)-\frac{m_2}{r_F^2}\right]\left[au-a^2(m_2-q_F)+\frac{m_2}{\rho_A^2}\right]$$

$$\cdot\, e^{iu(\sigma_F-\sigma_A-a\epsilon)/a}\,\Lambda^{(\bar{m})}\left((-q_F-\tfrac{u}{a})\theta_{bF}\right)$$

$$\cdot\,\Lambda^{(\bar{n})}\left((2m_2-q_F-\tfrac{u}{a})\theta_{bA}\right)$$

and

$$\bar{K}_{FA}^{(\bar{m},\bar{n})}(m_3=q_A+\ell_3 N_F\geq 0)=\left\{\frac{-N_F}{4\pi\rho_f U^2 r_{F0}}\right\}\frac{r_A}{a\sqrt{1+a^2 r_A^2}}\,e^{-im_3(2\sigma_F-a\epsilon)}$$

$$\cdot e^{+iq_A(\sigma_F-\sigma_A-a\epsilon)}\left\{C(0)D(0)-\frac{i}{\pi}\int_0^\infty[C(u)D(u)-C(-u)D(-u)]\frac{du}{u}\right\} \tag{9}$$

where

$$C(u)=\begin{cases} I_{m_3}(|u+a(m_3-q_A)|\rho_F)K_{m_3}(|u+a(m_3-q_A)|r_A) & \text{for } \rho_F\leq r_A \\ I_{m_3}(|u+a(m_3-q_A)|r_A)K_{m_3}(|u+a(m_3-q_A)|\rho_F) & \text{for } r_A<\rho_F \end{cases}$$

$$D(u)=\left[au+a^2(m_3-q_A)+\frac{m_3}{r_A^2}\right]\left[au+a^2(m_3-q_A)-\frac{m_3}{\rho_F^2}\right]$$

$$\cdot\, e^{-iu(\sigma_F-\sigma_A-a\epsilon)/a}\,\Lambda^{(\bar{m})}\left((q_A-\tfrac{u}{a})\theta_{bA}\right)$$

$$\cdot\,\Lambda^{(\bar{n})}\left((-2m_3+q_A-\tfrac{u}{a})\theta_{bF}\right)$$

The kernels have been programmed with proper consideration being given to evaluating the finite contributions of the Cauchy-type singularities in the u-integrations at $u=0$ and of the Hadamard-type higher order singularities in the ρ-integrations when $\rho \rightarrow r$.

THE NORMAL VELOCITIES

The LH sides of the integral equations represent the normal components of the velocity perturbations above that producing zero loading (lift) which corresponds to a rotating thin plate (i.e., without camber and thickness) lying on the helicoidal surface of pitch angle (advance angle)

$$\beta = \tan^{-1} \frac{U}{\Omega r}$$

where U = forward speed, r = radial location of the corresponding helix, and Ω = amplitude of angular velocity.

The perturbations considered are those due to (a) hull wake (non-uniform inflow), (b) blade camber, (c) incident flow angle, (d) the blade thicknesses which affect both steady and unsteady velocity field around both propellers of the CR system, (e) the effect of forward propeller race on the after propeller, and, finally, (f) the induction on the after propeller due to the viscous part of the forward propeller wake. Since the after propeller is located in the wake of the forward propeller and it operates in a real fluid, the velocity induction should include both the potential and viscous effects. In the absence of wake measurements in the plane of the after propeller when the forward propeller is in place, an approximate method based on the Kemp and Sears approach [16] has been utilized. The factors (a) to (e) inclusive are considered to be the potential part of the induction whereas (f) is due to the presence of viscosity.

The effects of these imposed flows on the blade are calculated separately and simply added together as allowed by linear theory.

(A) Hull Wake

The left-hand sides of the integral equations due to the wake contribution can be harmonically analyzed and written in the form

$$W(r,\Theta) = \sum_{q=0} V_n(r) e^{-iq\Theta}$$

where Θ can be expressed in terms of the moving coordinate system attached to each propeller by $\Theta_F = -\theta_{0F} + \Omega_F t$ and $\Theta_A = +\theta_{0A} - \Omega_A t$ for the case of the forward and after propeller, respectively, as shown in Figure 1. The normal wake velocities $V_n(r)$ can be determined from the harmonic analysis of the wake measurements, as shown in Reference [9]. After the trigonometric transformation

$$\theta_o = \sigma - \theta_b \cos\theta_\alpha$$

and application of the "lift operator" of order $\bar{m}$

$$\frac{1}{\pi} \int_0^\pi \Phi(\bar{m}) W(r,\Theta) d\theta_\alpha$$

the following expressions result for the left-hand sides of the pair of integral equations relating the unknown loadings with the given "downwash" at each propeller:

$$\frac{\bar{W}_A^{(q_A,\bar{m})}(r_A)}{U} = \frac{V_A^{(q_A)}(r_A)}{U} e^{-iq_A\sigma_{A_1}(\bar{m})(q_A\theta_{bA})}$$

for the after propeller, and (10)

$$\frac{\bar{W}_F^{(q_F,\bar{m})}(r_F)}{U} = \text{conj}\left[\frac{V_F^{(q_F)}(r_F)}{U} e^{-iq_F\sigma_{F_1}(\bar{m})(q_F\theta_{bF})}\right]$$

for the forward propeller. It should be noted that the factor $\exp(\pm q\Omega t)$ has been omitted from the above expressions.

(B) Incident Flow Angle

The velocities induced by the incident flow angle and camber effects are independent of time because the blades are considered rigid so that only the steady-state loadings will be affected.

For the flow angle (f) effects, the dimensionless perturbation

velocities after the application of the lift operator become:

$$\left(\frac{\bar{W}_F^{(0,\bar{m})}(r_F)}{U}\right)_f = -\sqrt{1+a^2 r_F^2}\left[\theta_{PF}(r_F)-\beta_F(r_F)\right]_I^{(\bar{m})}(0)$$

and (11)

$$\left(\frac{\bar{W}_A^{(0,\bar{m})}(r_A)}{U}\right)_f = -\sqrt{1+a^2 r_A^2}\left[\theta_{PA}(r_A)-\beta_A(r_A)\right]_I^{(\bar{m})}(0)$$

for the forward and after propellers, respectively, where θ_P is the blade pitch angle and β is the advance angle (hydrodynamic pitch angle) of the reference helicoidal surface (i.e., of zero loading).

(C) Propeller Camber

For the camber (c) effect of the forward propeller, the dimensionless velocity ratio after the application of the lift operator becomes

$$\left(\frac{\bar{W}_F^{(0,\bar{m})}(r_F)}{U}\right)_c = \frac{\sqrt{1+a^2 r_F^2}}{\pi c(r_F)}\int_0^{\pi} \Phi(\bar{m})\frac{\partial f(r_F,s_F)}{\partial s_F}\,d\varphi_\alpha \quad (12)$$

where

$f(r_F,s_F)$ = camberline ordinates as fraction of expanded chord length, measured from the face pitch line

$s_F = (1-\cos\varphi_\alpha)/2$, chordwise location non-dimensionalized on the basis of chord length $c(r_F)$

For the after propeller, the same expression is valid and only the subscript F must be replaced by A .

The evaluation of the integral of (12) is given in Reference [11] for arbitrary camber shape.

(D) Blade Thickness of Each Propeller on the Velocity Field of the Other

In addition to the disturbances of the velocity field about each propeller due to wake, its flow angle and camber, the disturbances considered are those due to the effects of the thickness of the blades of one propeller on the velocity incident on the other. These normal velocities on the LH side of the integral equations have been developed on the basis of "thin" body approximations.[12] Furthermore, it is assumed that the thickness distribution is approximated by a lenticular cross-section, an assumption which has been shown to be a good approximation for determining velocity and pressure [12,13] on a point in the neighborhood of an operating propeller as long as it is not a point on its blade and particularly near the leading edge. It should also be recalled that the velocity and pressure fields generated by an operating propeller even in a uniform inflow yield steady and unsteady components of the respective field. Thus although it is independent of time, the blade thickness produces both steady and unsteady components of the velocity field.

Following the same procedure as in Reference [12], it can be shown that the dimensionless velocity normal to the blades of the forward propeller induced by the after propeller thickness, with maximum thickness-chord ratio t_o/c, is given for $q_F=0$ by

$$\left(\frac{\bar{W}_F^{(0,\bar{m})}(r_F)}{U}\right)_{tA} = -\frac{4a^3 r_F N_A}{\pi^2\sqrt{1+a^2 r_F^2}} \int_{\rho_A} \frac{\rho_A}{\theta_{bA}} \sqrt{1+a^2\rho_A^2}\ \frac{t_o}{c}(\rho_A)$$

$$\cdot \int_0^\infty u(IK)_b F(u,\rho_A) R.P.\left[e^{iu(\sigma_A-\sigma_F+a\epsilon)/a}\ I^{(\bar{m})}\left(\frac{u}{a}\theta_{bF}\right)\right] du d\rho_A \quad (13)$$

where

$$(IK)_o = \begin{cases} I_o(u\rho_A)K_o(ur_F) & \text{for } \rho_A < r_F \\ I_o(ur_F)K_o(u\rho_A) & \text{for } r_F < \rho_A \end{cases}$$

$$F(u,\rho_A) = \frac{\sin\frac{u\theta_{bA}}{a} - \frac{u\theta_{bA}}{a}\cos\left(\frac{u\theta_{bA}}{a}\right)}{u^2}$$

$I_o(\ )$ and $K_o(\ )$ are modified Bessel functions of first and second kind of order zero

and for $q_F = 2\ell N_A$ where $\ell=1,2, \ldots$, by

$$\left(\frac{\bar{W}_F^{(2\ell N_A,\bar{m})}(r_F)}{U}\right)_{tA} = -\frac{4a^2 r_F N_A}{\pi^2\sqrt{1+a^2 r_F^2}}\, e^{-i\ell N_A(2\sigma_F - a\epsilon)} \cdot \int_{\rho_A} \frac{\rho_A}{\theta_{bA}}\sqrt{1+a^2\rho_A^2}\,\frac{t_o}{c}(\rho_A) \cdot \int_0^\infty F(u,\rho_A)[G(u)-G(-u)]\,du\,d\rho_A \quad (14)$$

where

$$G(u) = \left[au + \ell N_A\left(a^2 - \frac{1}{r_F^2}\right)\right] I_{\ell N_A}(|u+a\ell N_A|\rho_A) K_{\ell N_A}(|u+a\ell N_A|\, r_F) \cdot e^{iu(\sigma_A-\sigma_F+a\epsilon)/a}\, I^{(\bar{m})}\left((2\ell N_A + \frac{u}{a})\theta_{bF}\right)$$

for $\rho_A < r_F$. If $\rho_A > r_F$, these factors are interchanged in the modified Bessel functions.

The velocity normal to the blades of the after propeller induced by the forward propeller thickness is for $q_A=0$

$$\left(\frac{\bar{W}_A^{(0,\bar{m})}(r_A)}{U}\right)_{tF} = \frac{-4a^3 r_A N_F}{\pi^2\sqrt{1+a^2 r_A^2}} \int_{\rho_F} \frac{\rho_F}{\theta_{bF}}\sqrt{1+a^2\rho_F^2}\,\frac{t_o}{c}(\rho_F) \cdot \int_0^\infty u\,(IK)_o F(u,\rho_F)\,R.P.\left[e^{-iu(\sigma_A-\sigma_F+a\epsilon)/a}\, I^{(\bar{m})}\left(\frac{u\theta_{bA}}{a}\right)\right] du\,d\rho_F \quad (15)$$

where

$$(IK)_o = \begin{cases} I_o(u\rho_F)K_o(ur_A) & \text{for } \rho_F < r_A \\ I_o(ur_A)K_o(u\rho_F) & \text{for } r_A < \rho_F \end{cases}$$

$$F(u,\rho_F) = \frac{\sin\frac{u\theta_{bF}}{a} - \frac{u\theta_{bF}}{a}\cos\frac{u\theta_{bF}}{a}}{u^2}$$

and for $q_A = 2\ell N_F$, $\ell = 1, 2, \ldots$

$$\left(\frac{\bar{W}_A^{(2\ell N_F, \bar{m})}(r_A)}{U}\right)_{tF} = \frac{-4a^2 r_A N_F}{\pi^2\sqrt{1+a^2 r_A^2}} e^{-i\ell N_F(2\sigma_A + a\epsilon)}$$

$$\cdot \int_{\rho_F} \frac{\rho_F}{\theta_{bF}} \sqrt{1+a^2\rho_F^2}\ \frac{t_o}{c}(\rho_F)$$

$$\cdot \int_0^\infty F(u, \rho_F)[N(u) - N(-u)]du d\rho_F \quad (16)$$

where

$$N(u) = \left[au + \ell N_F\left(a^2 - \frac{1}{r_A^2}\right)\right] I_{\ell N_F}(|u + a\ell N_F|\rho_F) K_{\ell N_F}(|u + a\ell N_F| r_A)$$

$$\cdot e^{-iu(\sigma_A - \sigma_F + a\epsilon)/a} I^{(\bar{m})}\left((2\ell N_F + \frac{u}{a})\theta_{bA}\right)$$

for $\rho_F < r_a$. If $\rho_F > r_A$, these factors are interchanged in the modified Bessel functions.

(E) Effect of Forward Propeller Race on the After Propeller

Since the after propeller of the CR system operates in the wake of the forward propeller, special attention must be given in calculating the velocity induced by the forward propeller on the after propeller. As shown in Appendix A for the equal RPM case, the wake induction effect to be added to the downwash velocity $\bar{W}_A^{(q_A, \bar{m})}/U$ is given by

$$\frac{\Delta\bar{W}_A^{(0,\bar{m})}(r_A)}{U} = -\frac{N_F}{2\pi\rho_f U^2 r_{F0}} \frac{1}{\sqrt{1+a^2 r_A^2}}\left(ar_A - \frac{1}{ar_A}\right)\frac{1}{r_A}$$

$$\cdot L_F^{(0,\bar{n})}(r_A)\Lambda^{(\bar{n})}(0) I^{(\bar{m})}(0) \quad \text{for } q_A = 0 \quad (17)$$

and

$$\frac{\Delta\bar{W}_A^{(2N_F,\bar{m})}}{U} = -\frac{N_F}{2\pi\rho_f U^2 r_{F0}} \frac{1}{\sqrt{1+a^2 r_A^2}}\left(ar_A - \frac{1}{ar_A}\right)\frac{1}{r_A}$$

$$\cdot L_F^{(0,\bar{n})}(r_A)\Lambda^{(\bar{n})}(0) I^{(\bar{m})}(2N_F\theta_{bA}^r) e^{-iaN_F\epsilon} e^{-i2N_F\sigma_A^r} \quad \text{for } q_A = 2N_F \quad (18)$$

(F) Induction on the After Propeller Due to Viscous Wake of the Forward Propeller

Since the after propeller is located in the race of the forward propeller, it operates in a viscous fluid and hence the induced velocity on the after propeller should include both potential and viscous flow effects. The potential flow effects have been considered in the preceding divisions A through E of the present section. The viscous flow effects are determined approximately by following the Kemp and Sears approach[16] adapted to the CR system as shown in Appendix B.

The induced velocity at any appropriate frequency on the after propeller is

$$\left(\frac{\tilde{w}}{U}\right)^{(q,\bar{m})}_{vis.}(r_A) = \frac{u}{U}^{(q)}(r_A)e^{-iq\sigma^r}\, I^{(\bar{m})}(q\theta_b^r) \qquad (19)$$

after application of the lift-operator given by Eq.(7a),

where

$\frac{u}{U}^{(q)}(r_A)$ = nondimensional viscous wake velocity at midchord points on the after propeller at radial locations r_A and frequency q. This quantity is calculated according to Reference [16]. (See Appendix B.)

The other symbols have been defined previously.

SOLUTION OF THE PAIR OF INTEGRAL EQUATIONS

It is seen from Eqs.(5) and (6) that the loading on each propeller of the CR system is affected by all the harmonics of the inflow field. Here, however, the solution will be limited to the uniform inflow case. The viscous part will be treated separately and it will not be considered as participating in the iterative scheme which will be discussed later. The normal velocities in the potential flow case are due to the following contributors: camber (c), incident flow (f), steady and unsteady effects of the interactions between the two propellers (i.e., cross-coupling terms), the respective thicknesses of the two units of the CR system, and, finally, the effect of the forward propeller race on the after propeller.

(A) Potential Flow

Equation (5) becomes for each $\bar{m}$ and $\bar{n}$ for $q_F=0$

$$\left[\frac{\bar{W}_F^{(0)}(r_F)}{U}\right]_{c+f+tA} = \int_{\rho_F} L_F^{(0)}(\rho_F)\bar{K}'_{FF}(q_F=0)\,d\rho_F + \int_{\rho_A}\left\{L_A^{(0)}(\rho_A)\bar{K}_{AF}(m_a=0)+L_A^{(2N_A)}(\rho_A)\bar{K}_{AF}(m_a=N_A)+\ldots\right\}d\rho_A \tag{20a}$$

and for $q_F = 2N_A$

$$\left[\frac{\bar{W}_F^{(2N_A)}(r_F)}{U}\right]_{tA} = \int_{\rho_F} L_F^{(2N_A)}(\rho_F)\bar{K}'_{FF}(q_F=2N_A)\,d\rho_F + \int_{\rho_A}\left\{L_A^{(0)}(\rho_A)\bar{K}_{AF}(m_a=N_A)+L_A^{(2N_A)}(\rho_A)\bar{K}_{AF}(m_a=2N_A)+\ldots\right\}d\rho_A \tag{20b}$$

Equation (6) becomes for each $\bar{m}$ and $\bar{n}$, for $q_A = 0$

$$\left[\frac{\bar{W}_A^{(0)}(r_A)}{U}\right]_{c+f+tF} + \frac{\Delta\bar{W}_A^{(0)}(r_A)}{U} = \int_{\rho_F} \left\{ L_F^{(0)}(\rho_F)\bar{K}_{FA}(m_3=0) + L_F^{(2N_F)}(\rho_F)\bar{K}_{FA}(m_3=N_F) + \ldots \right\} d\rho_F + \int_{\rho_A} L_A^{(0)}(\rho_A)\bar{K}'_{AA}(q_A=0)\, d\rho_A \qquad (21a)$$

and for $q_A = 2N_F$

$$\left[\frac{\bar{W}_A^{(2N_F)}(r_A)}{U}\right]_{tf} + \frac{\Delta\bar{W}_A^{(2N_F)}(r_A)}{U} = \int_{\rho_F} \left\{ L_F^{(0)}(\rho_F)\bar{K}_{FA}(m_3=N_F) + L_F^{(2N_F)}(\rho_F)\bar{K}_{FA}(m_3=2N_F) + \ldots \right\} d\rho_F + \int_{\rho_A} L_A^{(2N_F)}(\rho_A)\bar{K}'_{AA}(q_A=2N_F)\, d\rho_A \qquad (21b)$$

where

$$\bar{K}'_{FF} = \sum_{m_1=-\infty}^{\infty} \bar{K}_{FF}$$

$$\bar{K}'_{AA} = \sum_{m_4=-\infty}^{\infty} \bar{K}_{AA}$$

and so forth, for the higher frequencies.

Even in this simplified problem, a direct solution of the equations is impracticable; therefore an iteration procedure must be devised. It is assumed at first that the effect of the after propeller on the forward propeller (except for the thickness effect) is small and hence the second terms on the RH of Eqs.(20a) and (20b) may be omitted. Having obtained the loadings for the forward propeller at any required frequency, the loadings on the after propeller in the presence of the forward propeller can now be evaluated by means of Eqs.(21a) and (21b). Then the loadings of the forward and after propellers obtained through this first approximation will be incorporated in the next iteration by using the full equations (20a,b) and equations (21a,b). The calculation procedure will be described later in

detail in the section "Numerical Solution," but the iteration scheme is given below for the i^{th} iteration for a CR system with equal number of blades, $N_F=N_A=N$, and for one with unequal number, $N_F \neq N_A$, neither being an integer multiple of the other.

CASE #1: $N_F=N_A=N$

i-iteration

$$1)\quad L_{F_i}^{(0,\bar{n})}(\rho_F) = [\bar{K}'_{FF}(q_F=0)]^{-1}\left\{\left(\frac{\bar{W}_F^{(0,\bar{m})}(r_F)}{U}\right)_{c+f}+\left(\frac{\bar{W}_F^{(0,\bar{m})}(r_F)}{U}\right)_{tA}\right.$$

$$-\sum_{\rho_A}\left[L_{A_{i-1}}^{(0,\bar{n})}\bar{K}_{AF}^{(\bar{m},\bar{n})}(m_a=0,q_F=0)\right.$$

$$+L_{A_{i-1}}^{(2N,\bar{n})}\bar{K}_{AF}^{(\bar{m},\bar{n})}(m_a=N,\ q_F=0)$$

$$\left.\left.+L_{A_{i-1}}^{(4N,\bar{n})}\bar{K}_{AF}^{(\bar{m},\bar{n})}(m_a=2N,\ q_F=0)\right]\right\} \qquad (22)$$

$$2)\quad L_{F_i}^{(2N,\bar{n})}(\rho_F) = [\bar{K}'_{FF}(q_F=-2N)]^{-1}\left\{\left(\frac{\bar{W}_F^{(2N,\bar{m})}(r_F)}{U}\right)_{tA}\right.$$

$$-\sum_{\rho_A}\left[L_{A_{i-1}}^{(0,\bar{n})}\bar{K}_{AF}^{(\bar{m},\bar{n})}(m_a=N,\ q_F=2N)\right.$$

$$+L_{A_{i-1}}^{(2N,\bar{n})}\bar{K}_{AF}^{(\bar{m},\bar{n})}(m_a=2N,\ q_F=2N)$$

$$\left.\left.+L_{A_{i-1}}^{(4N,\bar{n})}\bar{K}_{AF}^{(\bar{m},\bar{n})}(m_a=3N,q_F=2N)\right]\right\} \qquad (23)$$

$$3)\quad L_{F_i}^{(4N,\bar{n})}(\rho_F) = \left[\bar{K}'_{FF}(q_F=-4N)\right]^{-1}\left\{\left(\frac{\bar{W}_F^{(4N,\bar{m})}(r_F)}{U}\right)_{tA}\right.$$

$$-\sum_{\rho_A}\left[L_{A_{i-1}}^{(0,\bar{n})}\bar{K}_{AF}^{(\bar{m},\bar{n})}(m_a=2N,\ q_F=4N)\right.$$

$$+L_{A_{i-1}}^{(2N,\bar{n})}\bar{K}_{AF}^{(\bar{m},\bar{n})}(m_a=3N,\ q_F=4N)$$

$$\left.\left.+L_{A_{i-1}}^{(4N,\bar{n})}\bar{K}_{AF}^{(\bar{m},\bar{n})}(m_a=4N,\ q_F=4N)\right]\right\} \qquad (24)$$

and

$$4)\quad L_{A_i}^{(0,\bar{n})}(\rho_A) = [\bar{K}'_{AA}(q_A=0)]^{-1}\left\{\left(\frac{\bar{W}_A^{(0,\bar{m})}(r_A)}{U}\right)_{c+f}+\left(\frac{\bar{W}_A^{(0,\bar{m})}(r_A)}{U}\right)_{tF}+\left(\frac{\Delta\bar{W}_A^{(0,\bar{m})}(r_A)}{U}\right)\right.$$

$$-\sum_{\rho_F}\left[L_{F_i}^{(0,\bar{n})}\bar{K}_{FA}^{(\bar{m},\bar{n})}(m_3=0,\ q_A=0)\right.$$

$$+L_{F_i}^{(2N,\bar{n})}\bar{K}_{FA}^{(\bar{m},\bar{n})}(m_3=N,\ q_A=0)$$

$$\left.\left.+L_{F_i}^{(4N,\bar{n})}\bar{K}_{FA}^{(\bar{m},\bar{n})}(m_3=2N,\ q_A=0)\right]\right\} \qquad (25)$$

$$5)\quad L_{A_i}^{(2N,\bar{n})}(\rho_A) = [\bar{K}'_{AA}(q_A=2N)]^{-1}\left\{\left(\frac{\bar{W}_A^{(2N,\bar{m})}(r_A)}{U}\right)_{tf}+\left(\frac{\Delta\bar{W}_A^{(2N,\bar{m})}(r_A)}{U}\right)\right.$$

$$-\sum_{\rho_F}\left[L_{F_i}^{(0,\bar{n})}\bar{K}_{FA}^{(\bar{m},\bar{n})}(m_3=N,\ q_A=2N)\right.$$

$$+L_{F_i}^{(2N,\bar{n})}\bar{K}_{FA}^{(\bar{m},\bar{n})}(m_3=2N,\ q_A=2N)$$

$$\left.\left.+L_{F_i}^{(4N,\bar{n})}\bar{K}_{FA}^{(\bar{m},\bar{n})}(m_3=3N,\ q_A=2N)\right]\right\} \qquad (26)$$

$$6)\quad L_{A_i}^{(4N,\bar{n})}(\rho_A) = [\bar{K}'_{AA}(q_A=4N)]^{-1}\left\{\left(\frac{\bar{W}_A^{(4N,\bar{m})}(r_A)}{U}\right)_{tf}+\left(\frac{\Delta\bar{W}_A^{(4N,\bar{m})}(r_A)}{U}\right)\right.$$

$$-\sum_{\rho_F}\left[L_{F_i}^{(0,\bar{n})}\bar{K}_{FA}(m_3=2N,\ q_A=4N)\right.$$

$$+L_{F_i}^{(2N,\bar{n})}\bar{K}_{FA}^{(\bar{m},\bar{n})}(m_3=3N,\ q_A=4N)$$

$$\left.\left.+L_{F_i}^{(4N,\bar{n})}\bar{K}_{FA}^{(\bar{m},\bar{n})}(m_3=4N,\ q_A=4N)\right]\right\} \qquad (27)$$

CASE #2 $N_F \neq N_A$

$$1)\quad L_{F_i}^{(0,\bar{n})}(\rho_F) = [\bar{K}'_{FF}(q_F = 0)]^{-1}\left\{\left(\frac{\bar{W}_F^{(0,\bar{m})}(r_F)}{U}\right)_{c+f+tA} - \sum_{\rho_A}\left[L_{A_{i-1}}^{(0,\bar{n})}\bar{K}_{AF}^{(\bar{m},\bar{n})}(m_a = 0,\ q_F = 0)\right]\right\} \tag{28}$$

$$2)\quad L_{F_i}^{(2N_A,\bar{n})}(\rho_F) = [\bar{K}'_{FF}(q_F = -2N_A)]^{-1}\left\{\left(\frac{\bar{W}_F^{(2N_A,\bar{n})}(r_F)}{U}\right)_{tA} - \sum_{\rho_A}\left[L_{A_{i-1}}^{(0,\bar{n})}\bar{K}_{AF}^{(\bar{m},\bar{n})}(m_a = N_A, q_F = 2N_A)\right]\right\} \tag{29}$$

$$3)\quad L_{A_i}^{(0,\bar{n})}(\rho_A) = [\bar{K}'_{AA}(q_A=0)]^{-1}\left\{\left(\frac{\bar{W}_A^{(0,\bar{m})}(r_A)}{U}\right)_{c+f+tF} + \left(\frac{\Delta\bar{W}_A^{(0,\bar{m})}(r_A)}{U}\right) - \sum_{\rho_F}\left[L_{F_i}^{(0,\bar{n})}\bar{K}_{FA}^{(\bar{m},\bar{n})}(m_3 = 0,\ q_A = 0)\right]\right\} \tag{30}$$

$$4)\quad L_{A_i}^{(2N_F,\bar{n})}(\rho_A) = [\bar{K}'_{AA}(q_A=2N_F)]^{-1}\left\{\left(\frac{\bar{W}_A^{(2N_F,\bar{m})}(r_A)}{U}\right)_{tF} + \left(\frac{\Delta\bar{W}_A^{(2N_F,\bar{m})}(r_A)}{U}\right) - \sum_{\rho_F}\left[L_{F_i}^{(0,\bar{n})}\bar{K}^{(\bar{m},\bar{n})}(m_3 = N_F,\ q_A = 2N_F)\right]\right\} \tag{31}$$

where

$$K'_{FF}(q_F) = \sum_{m=-\infty}^{\infty} K_{FF}(q_F, m)$$

$$K'_{AA}(q_A) = \sum_{m=-\infty}^{\infty} K_{AA}(q_A, m)$$

When subscript $i-1=0$, then the quantity under consideration must be taken to be zero.

It is to be noted that, in contrast to the case of equal number of blades for the two propellers of the CR system, when the propellers have

an unequal number of blades, $N_A \neq N_F$, the series representing the cross-coupling terms due to the interaction effects are more limited. As will be shown later, for this case there is no unsteady loading L_F on the forward propeller at frequency $2N_F$ and no unsteady loading L_A on the after propeller at frequency $2N_A$. It should be kept in mind that the iteration scheme has been restricted to the lowest possible frequencies of the interacting CR system. It will be easily generalized by means of Eqs.(5) and (6) by varying parameters ℓ_1, ℓ_2, ℓ_3, ℓ_4 (all integers) to other values than those already used (0, ±1). The iterations will continue until the values of the loadings will be stabilized, i.e., they will not change for consecutive iterations.

(B) Viscous Flow Effects

The last iteration establishes the value of the pitch of the reference surfaces for both propellers of the CR system. At this stage, the viscous effect on the induced velocity of the after propeller is calculated by means of Eq.(19) at the desired frequency. The loadings of the after propeller are determined through the solution of the integral equation relating the known upwash with the unknown blade loading.

CASE #1 $N_F = N_A = N$

$$L_A^{(2N,\bar{n})}(\rho_A) = \left[\bar{K}'_{AA}(q = 2N)\right]^{-1}\left(\frac{W}{U}^{(2N,\bar{m})}(r_A)\right)_{vis.} \tag{32a}$$

and

$$L_A^{(4N,\bar{n})}(\rho_A) = \left[\bar{K}'_{AA}(q = 4N)\right]^{-1}\left(\frac{W}{U}^{(4N,\bar{m})}(r_A)\right)_{vis.} \tag{32b}$$

CASE #2 $N_F \neq N_A$ (Neither one is an integer multiple of the other.)
In this case

$$L_A^{(2N_F,\bar{n})}(\rho_A) = \left[\bar{K}'_{AA}(q=2N_F)\right]^{-1}\left(\frac{W}{U}^{(2N_F,\bar{m})}(r_A)\right)_{vis.} \tag{33}$$

The viscous flow results should be added to the potential values at the corresponding frequencies to determine the combined effects. The same results can be obtained by adding the viscous inductions to Eqs.(26) and (27) for the case $N_A = N_F = N$ and Eq.(31) for $N_F \neq N_A$ at the last iteration of the numerical scheme, so that the final values of blade loadings will be determined.

PROPELLER LOADING AND RESULTING HYDRODYNAMIC FORCES AND MOMENTS

Propeller Loading

Once the values of $L^{(q,\bar{n})}(r)$, the spanwise loading components, or coefficients of the chordwise distribution, are obtained, the spanwise loading distribution $L^{(q)}(r)$ is determined as:[9,10]

$$L^{(q)}(r) = \int_0^{\pi} \sum_{\bar{n}=1}^{\bar{n}max} L^{(q,\bar{n})}(r)\Theta(\bar{n})\sin\theta_\alpha d\theta_\alpha \qquad (34)$$

where $\Theta(\bar{n})$ = chordwise modes. Because the interaction phenomenon introduces an angle of attack even in the steady-state case $\Theta(\bar{n})$ is taken as the complete Birnbaum series which has the proper leading edge singularity and satisfies the Kutta condition at the trailing edge. In this case it can be shown that

$$L^{(q)}(r) = L^{(q,1)}(r) + \frac{1}{2} L^{(q,2)}(r) \qquad (35)$$

Hydrodynamic Forces and Moments

The principal components of these forces and moments which are evaluated for each member of the CR system are listed below and shown in Figure 2 for a RH propeller with the sign convention adopted.

Forces: F_x = thrust (x-direction)

F_y and F_z = horizontal and vertical components, respectively, of the bearing forces

Moments: Q_x = torque about the x-axis

Q_y and Q_z = bending moments about the y- and z-axis, respectively.

(Subscripts F and A added to these symbols will designate forward and after propeller cases.)

The elementary forces and moments can be determined by resolving the chordwise loadings, acting on an elementary radial strip, normal to the strip and taking the corresponding moments about any axis as in Reference [9].

Thus the elementary forces acting at radius r of an N-bladed propeller will be given by

$$\Delta F_x = \sum_{n=1}^{N} L^{(q)}(r) e^{iq(\Omega t+\bar{\theta}_n)} \cos\theta_p(r)\Delta r$$

$$\Delta F_y = \sum_{n=1}^{N} L^{(q)}(r) e^{iq(\Omega t+\bar{\theta}_n)} \sin\theta_p(r)\cos(\Omega t-\varphi_o+\bar{\theta}_n)\Delta r \qquad (36)$$

$$\Delta F_z = -\sum_{n=1}^{N} L^{(q)}(r) e^{iq(\Omega t+\bar{\theta}_n)} \sin\theta_p(r)\sin(\Omega t-\varphi_o+\bar{\theta}_n)\Delta r$$

where $\theta_p(r)$ is the geometric pitch angle at radius r and $\bar{\theta}_n = 2\pi(n-1)/N$, $n=1, 2, \ldots, N$. The elementary moments will be given by

$$\Delta Q_x = -\sum_{n=1}^{N} rL^{(q)}(r) e^{iq(\Omega t+\bar{\theta}_n)} \sin\theta_p(r)\Delta r$$

$$\Delta Q_y = \sum_{n=1}^{N} rL^{(q)}(r) e^{iq(\Omega t+\bar{\theta}_n)} \cos\theta_p(r)\cos(\Omega t-\varphi_o+\theta_n)\Delta r \qquad (37)$$

$$\Delta Q_z = -\sum_{n=1}^{N} rL^{(q)}(r) e^{iq(\Omega t+\bar{\theta}_n)} \cos\theta_p(r)\sin(\Omega t-\varphi_o+\theta_n)\Delta r$$

The summation over all the blades of a propeller involves

1) for thrust and torque

$$\sum_{n=1}^{N} e^{iq\bar{\theta}_n} = \begin{cases} N \text{ when } q=nN,\ n=0,1,2\ \ldots \\ 0 \text{ for all other } q \end{cases} \qquad (38)$$

2) for transverse forces and bending moments

$$\sum_{n=1}^{N} e^{i(q\pm1)\bar{\theta}_n} = \begin{cases} N \text{ when } q=nN\pm1,\ n=0,1,2\ \ldots \\ 0 \text{ for all other } q \end{cases} \qquad (39)$$

It is thus evident that in the steady-state case ($q=0$) thrust and torque from each propeller will be present (see Eq.38) whereas, since the condition under consideration is that of uniform inflow into the forward propeller, there will be no transverse forces and bending moments (see Eq.39).

This will be so whether the propellers are of equal or unequal number of blades.

As has been shown, the interaction phenomenon induces unsteady loadings on both units of the CR system. In the case of equal blade number, those on the forward propeller are $L_F^{(2\ell N)}(r_F)$, on the after propeller, $L_A^{(2\ell N)}(r_A)$. As seen from Eqs.(38) and (39), both propellers generate thrust and torque at frequencies $q=2\ell N$, $\ell=1, 2, \ldots$, which correspond to blade-blade crossing frequency for such propellers, and no unsteady transverse bearing forces and moments since no combination of integers ℓ and n can satisfy the relation $(2\ell-n)N = \mp 1$.

In the case of unequal blade number, $N_A \neq N_F$, the unsteady loadings on the forward propeller are at frequencies $q_F=2\ell_1 N_A$ and $2\ell_2 N_F$ and on the after propeller at $q_A=2\ell_3 N_F$ and $2\ell_4 N_A$. The criterion for thrust and torque, Eq.(38), yields

$$\begin{aligned} q_F &= 2\ell_1 N_A = n_1 N_F \\ q_F &= 2\ell_2 N_F = n_2 N_F \\ q_A &= 2\ell_3 N_F = n_3 N_A \\ q_A &= 2\ell_4 N_A = n_4 N_A \end{aligned} \tag{38a}$$

and the criterion for transverse forces and bending moments, Eq.(39), yields

$$\begin{aligned} q_F &= 2\ell_1 N_A = n_1 N_F \mp 1 \\ q_F &= 2\ell_2 N_F \neq n_2 N_F \mp 1 \\ q_A &= 2\ell_3 N_F = n_3 N_A \mp 1 \\ q_A &= 2\ell_4 N_A \neq n_4 N_A \mp 1 \end{aligned} \tag{39a}$$

The conditions of (38a) for thrust and torque are always satisfied for frequency $q=q_F=q_A$ by choosing $\ell_1=\ell_4=mN_F$, $\ell_2=\ell_3=mN_A$, $m=1, 2, \ldots$, so that $q=2mN_AN_F$, i.e., the so-called blade-blade crossing frequency and multiples thereof. Equation (38a) can also be satisfied at lower frequencies (1) if $N_A=kN_F$, k being an integer, in which case choosing $\ell_1 k=\ell_2=\ell_3=\ell_4 k$ yields $q=2mkN_F$, and (2) if N_A and N_F are both even numbers, in which case, $q=mN_AN_F$. In the latter two cases the conditions of (39a) for transverse forces and moments are obviously not satisfied.

When $N_A \neq kN_F$ and N_A and N_F are not both even numbers, the CR system generates thrust and torque only at $q=2mN_AN_F$ (blade-blade crossing frequencies).

The conditions of (39a) are satisfied for

$$q = q_F \mp 1 = 2\ell_1 N_A \mp 1 = n_1 N_F$$

$$q = q_A \pm 1 = 2\ell_3 N_F \pm 1 = n_3 N_A$$

since $2\ell_1 N_A + 2\ell_3 N_F = n_3 N_A + nN_F$ is possible. The frequencies at which side forces and bending moments of the CR system occur are

$$q = 2\ell_1 N_A \mp 1 = 2\ell_3 N_F \pm 1$$

from which $2\ell_1 N_A = 2\ell_3 N_F \pm 2$.

An easy way of determining the frequencies for alternating forces and moments is to write out the sequence of numbers which are integer multiples of twice the blade number. For example, for 3 and 5 blades

3: 6 12 18 24 30 ...

5: 10 20 30 ...

The frequencies for side forces will be the mean of any pair of numbers in the two sequences which differ by 2, in this case 11, 19 ... . The frequencies for thrust and torque will be the mean of any pair of numbers which are alike, in this case 30, 60 ... . For 6 and 4 blades, the two lowest frequencies will be 24 and 48 for thrust and torque. (There is no side force in this case.)

Another derivation of the frequencies of the alternating forces developed by interactions between a pair of counterrotating propellers in a uniform inflow is given by Reference [14] with the same results.

On the basis of the preceding discussion, the total forces and moments are obtained from Eqs.(36) and (37) as

1) For thrust and torque

$$(F_x)_F = N_F r_o e^{iq\Omega t} \int_o^1 L_F^{(q)}(r_F)\cos\theta_p(r_F)\,dr_F$$

$$(F_x)_A = N_A r_o e^{iq\Omega t} \int_o^1 L_A^{(q)}(r_A)\cos\theta_p(r_A)\,dr_A \qquad (40)$$

$$(Q_x)_F = -N_F r_o^2 e^{iq\Omega t} \int_o^1 L_F^{(q)}(r_F)\sin\theta_p(r_F)\,r_F\,dr_F$$

$$(Q_x)_A = -N_A r_o^2 e^{iq\Omega t} \int_o^1 L_A^{(q)}(r_A)\sin\theta_p(r_A)\,r_A\,dr_A \qquad (41)$$

where q=0 for steady state, and the lowest frequency of the alternating thrust and torque is

$q = 2kN_F$ when $N_A = kN_F$, k=1, 2, ...

$q = N_A N_F$ when $N_A \neq N_F$ and both are even numbers

$q = 2N_A N_F$ for all other $N_A \neq N_F$

2) For transverse bearing forces and bending moments when $N_A \neq N_F$ and N_A and N_F are not both even numbers or multiples of each other:

$$(F_y)_F = 0.5N_F r_o e^{i(q_F \mp 1)\Omega t} \int_o^1 \sum_{\bar{n}} L_F^{(q_F,\bar{n})}(r_F)\Lambda^{(\bar{n})}(\pm\theta_{b_F}^r)\sin\theta_p(r_F)\,dr_F$$

$$(F_z)_F = \mp i(F_y)_F \qquad (42)$$

$$(F_y)_A = 0.5N_A r_o e^{i(q_A \pm 1)\Omega t} \int_o^1 \sum_{\bar{n}} L_A^{(q_A,\bar{n})}(r_A)\Lambda^{(\bar{n})}(\mp\theta_{b_A}^r)\sin\theta_p(r_A)\,dr_A$$

$$(F_z)_A = \pm i(F_y)_A \qquad (43)$$

$$(Q_y)_F = \frac{N_F}{2} r_o^2 e^{i(q_F \mp 1)\Omega t} \int_o^1 \sum_{\bar{n}} L_F^{(q_F,\bar{n})}(r_F)\, r_F \Big\{\Lambda^{(\bar{n})}(\pm\theta_{b_F}^r)\cos\theta_p(r_F)\,dr_F$$

$$\mp i\theta_{b_F}^r \sin\theta_p(r_F)\tan\theta_p(r_F)\Lambda_1^{(\bar{n})}(\pm\theta_{b_F}^r)\Big\}dr_F$$

$$(Q_z)_F = \mp i (Q_y)_F \tag{44}$$

$$(Q_y)_A = \frac{N_A}{2} r_o^2 e^{i(q_A \pm 1)\Omega t} \int_0^1 \sum_{\bar{n}} L_A^{(q_A,\bar{n})}(r_A)\, r_A \Big\{ \Lambda^{(\bar{n})}(\mp\theta_{b_A}^r)\cos\theta_p(r_A) \pm i\theta_{b_A}^r \sin\theta_p(r_A)\tan\theta_p(r_A)\Lambda_1^{(\bar{n})}(\mp\theta_{b_A}^r)\Big\} dr_A$$

$$(Q_z)_A = \pm i (Q_y)_A \tag{45}$$

where $\Lambda^{(\bar{n})}(x)$ is defined in Eq.(7b)

and $\Lambda_1^{(\bar{n})}(x) = \frac{1}{\pi}\int_0^{\pi} \Theta(\bar{n}) \sin\theta_\alpha \cos\theta_\alpha e^{-ix\cos\theta_\alpha} d\theta_\alpha$. [See Refs. 9, 10.]

The upper signs (at $q=q_F-1=q_A+1$) are used when $N_A > N_F$, and the lower signs (at $q=q_F+1=q_A-1$) are used when $N_A < N_F$, and $q_F = 2\ell_1 N_A$ and $q_A = 2\ell_3 N_F$ where ℓ_1 and ℓ_3 must satisfy the condition $2\ell_1 N_A = 2\ell_3 N_F \pm 2$.

It is to be noted that $r_o = r_{Fo}$ = forward propeller radius and r_A and r_F are fractions of r_{Fo}, and that finally the real parts of the forces and moments are to be taken.

Blade Bending Moment

Following References [9] & [10], the blade bending moment about the face pitch line at any radius r_j of a blade of the forward or after propeller is calculated from the spanwise loading $L^{(q)}(r)$ at any shaft frequency q as

$$M_b^{(q)} = r_o^2 e^{iq\Omega t} \int_{r_j}^1 L^{(q)}(r)\cos[\theta_p(r) - \theta_p(r_j)](r-r_j)\, dr \tag{46}$$

The instantaneous blade bending moment distribution as the blades swing around the shaft is

$$M_b = \mathrm{Re} \sum_q M_b^{(q)} e^{iq\Omega t} \tag{47}$$

Here $q=q_F$ for the forward propeller and $q=q_A$ for the after propeller.

NUMERICAL PROCEDURE

On the basis of the theoretical procedures outlined in the preceding sections, a numerical approach has been established and adapted to the CDC-6600 or 7600, or Cyber 176 high-speed digital computer. The program furnishes in the case of uniform inflow to the forward propeller, (a) the steady and time-dependent blade loadings, (b) the corresponding hydrodynamic forces and moments, and (c) the blade bending moment about the face-pitch line at any radius.

The expressions for the kernel functions given by Eqs.(7-9), those for the normal velocities on the left-hand sides of the integral equations given by Eqs.(10-18) (for the potential flow case), or (10-19) (for the combined potential and viscous flow effects), together with the pair of integral equations (20a,20b) and (21a,21b) constitute the desired working form. The computer program prepares all the necessary information for the execution of the suggested iteration procedure. Before conducting any calculations, a preliminary numerical investigation is performed with the sole purpose to establish the pitch of the helicoidal reference surface, around which the perturbation method is applied.[8,9,15]

From experience gained in a series of calculations utilizing the program developed for a CR system, it was found that the "advance angle," which is related to the pitch of the reference helicoidal surface,[9,10,15] is a very sensitive parameter and that small changes in values have a noticeable effect on the resulting hydrodynamic forces and moments. It was also found that time-dependent terms which are involved in calculating the steady-state hydrodynamic forces and moments (see iterative procedures [Eqs.22-31]) have insignificant effects and hence can be ignored at the first stage of this investigation. Furthermore, from experiments conducted at the David W. Taylor Naval Ship R&D Center with the purpose to establish the "open water" characteristics of a CR system, it was also noticed that each unit of the CR system operates with its own advance coefficient which is a little different in value from that of the coupled system. All these factors have been taken into consideration in establishing the iteration procedure.

On the basis of these observations the computer program is divided into

the following two parts:

(A) Auxiliary calculations with the sole purpose of establishing the pitch of the reference helicoidal surface.

(B) Final calculations where the complete interaction between the units of the CR system is taken into account.

PART A comprises the following steps:

1) Calculations of the inverses of the self-induction kernels

$$[K_{FF}]^{-1} \quad \text{and} \quad [K_{AA}]^{-1}$$

i.e., when both loading and control points are on the same unit of the CR system. They are evaluated at $a_A=a_F=a_0=\frac{\pi}{J_s}$ where J_s = advance coefficient of the CR system.

2) Determination of the inflow velocity field at its own advance coefficient which is very close to the value of J_s. It should be kept in mind that the inflow field remains unchanged during the iteration which will be discussed in Step #3. Sometimes a slight adjustment of the inflow field can bring results for $\bar{K}_T$ and $\bar{K}_Q$ in better agreement with experiments.

3) Calculations of the cross-coupling terms K_{AF} and K_{FA} are performed at values of $a=\frac{\pi}{J}$ determined by an iterative procedure. In this step only the steady state loadings are considered. The advance angle at each iteration is determined through the expression

$$a^{(i)} = \frac{\Omega r_o}{U^{(i)}} \tag{48}$$

where $U^{(i)}= U+u_i$; U = ship speed, and u_i = induction speed due to interacting lifting surfaces. For simplicity, the value at $0.7r_o$ is taken as the representative value of $U^{(i)}$ at the i^{th} iteration. With these values of $a_F^{(i)}$ and $a_A^{(i)}$, the cross-coupling kernels $K_{AF}^{(i)}$ and $K_{FA}^{(i)}$ and $\Delta\bar{W}_A/U$ (correction term) are calculated and thus the steady state loadings $L_F^{(0,\bar{n})}$ and $L_A^{(0,\bar{n})}$ and the corresponding thrust and torque are determined.

This iterative procedure will be terminated when the values of thrust and torque converge to their final values. We start at assumed values of $a_F=a_A=a_0$ of the system and after 4-5 iterations, the values of $\bar{K}_T$ and $\bar{K}_Q$ are stabilized.

If an adjustment of the inflow field is required so as to bring the results of $\bar{K}_T$ and $\bar{K}_Q$ in better agreement with existing measurements, this part can be achieved within 2 or 3 iterations with an additional 2-3 minutes of execution time.

Note while performing calculations for the inflow field for the 4-0-4 and 4-0-5 CR system, it was found that the appropriate values for a_F and a_A are the following:

For the 4-0-4: $J_F = 1.12$, $J_A = 1.08$ or $\begin{cases} a_F = 2.799 = 0.98a_o \\ a_A = 2.913 = 1.02a_o \end{cases}$

For the 4-0-5: $J_F = 1.13$, $J_A = 1.11$ or $\begin{cases} a_F = 2.756 = 0.96a_o \\ a_A = 2.856 = a_o \end{cases}$

where $a_o = \frac{\pi}{J_s}$ and J_s = advance coefficient of the CR system.

PART B

The final values of the advance angles $a_F^{(i)}$ and $a_A^{(i)}$ being thus established, the complete interaction problem is now considered. This part of the program takes into account the contributions from the steady and unsteady loadings and it is subdivided into the following:

a) Calculate all unsteady loadings by utilizing the steady state cross-coupling terms determined in PART A.

b) Perform iterations by taking into consideration all the contributions from steady and unsteady loadings.

The coding of the two parts, A and B, and their subdivisions, will be clarified to the reader by the following Tables 1 and 2.

TABLE 1

CASE $N_A = N_F = N$

PART A

1. Calculate inversion of self-induction kernels using $a_o = \frac{\pi}{J_s}$ with J_s of the system.

$$[\bar{K}_{FF}]^{-1}(q_F=0)$$

$$[\bar{K}_{FF}]^{-1}(q_F= -2N)$$

$$[\bar{K}_{FF}]^{-1}(q_F= -4N)$$

$$[\bar{K}_{AA}]^{-1}(q_A=0)$$

$$[\bar{K}_{AA}]^{-1}(q_A= 2N)$$

$$[\bar{K}_{AA}]^{-1}(q_A= 4N)$$

2. Steady loadings only

Uncoupled:

$$L_F^{(0,\bar{n})}(\rho_F) = [\bar{K}_{FF}(q_F=0)]^{-1}\left\{\left(\frac{\bar{W}_F^{(0,\bar{m})}}{U}\right)_{c+f}\right\}$$

$$L_A^{(0,\bar{n})}(\rho_A) = [\bar{K}_{AA}(q_A=0)]^{-1}\left\{\left(\frac{\bar{W}_A^{(0,\bar{m})}}{U}\right)_{c+f}\right\}$$

Iterations:

$$L_F^{(0,\bar{n})}(\rho_F) = [\bar{K}_{FF}(q_F=0)]^{-1}\left\{\left(\frac{\bar{W}_F^{(0,\bar{m})}}{U}\right)_{c+f+t_A} - \sum_{\rho_A}\left[L_A^{(0,\bar{n})}\bar{K}_{AF}^{(\bar{m},\bar{n})}(m_2=0,\ q_F=0)\right]\right\}$$

$$L_A^{(0,\bar{n})}(\rho_A) = [\bar{K}_{AA}(q_A=0)]^{-1}\left\{\left(\frac{\bar{W}_A^{(0,\bar{m})}}{U}\right)_{c+f+t_A} + \Delta\ \frac{\bar{W}_A^{(0,\bar{m})}}{U} - \sum_{\rho_F}\left[L_F^{(0,\bar{n})}\bar{K}_{FA}^{(\bar{m},\bar{n})}(m_3=0, q_A=0)\right]\right\}$$

From induced velocity, determine new a_F, a_A, utilizing Eq.(48) and recalculate the cross-coupling kernels $\bar{K}_{AF}$, $\bar{K}_{FA}$, and $\Delta\ \frac{\bar{W}_A^{(0,\bar{m})}}{U}$.

[Cont'd]

Table 1 (Cont'd)

PART B

a) Unsteady loadings

$$L_F^{(2N,\bar{n})}(\rho_F) = [\bar{K}'_{FF}(q_F = -2N)]^{-1}\left\{\left(\frac{\bar{W}_F^{(2N,\bar{m})}}{U}\right)_{t_A} - \sum_{\rho_A} L_A^{(0,\bar{n})}\bar{K}_{AF}^{(\bar{m},\bar{n})}(m_2=N, q_F=2N)\right\}$$

$$L_F^{(4N,\bar{n})}(\rho_F) = [\bar{K}'_{FF}(q_F = -4N)]^{-1}\left\{\left(\frac{\bar{W}_F^{(4N,\bar{m})}}{U}\right)_{t_A} - \sum_{\rho_A} L_A^{(0,\bar{n})}\bar{K}_{AF}^{(\bar{m},\bar{n})}(m_2=2N, q_F=4N)\right\}$$

$$L_A^{(2N,\bar{n})}(\rho_A) = [\bar{K}'_{AA}(q_A = 2N)]^{-1}\left\{\left(\frac{\bar{W}_A^{(2N,\bar{m})}}{U}\right)_{t_F} - \sum_{\rho_F} L_F^{(0,\bar{n})}\bar{K}_{FA}^{(\bar{m},\bar{n})}(m_3=N,\ q_A=2N)\right.$$

$$\left. + \left(\frac{\Delta\bar{W}_A}{U}\right)^{(2N,\bar{m})}_{\text{due to steady loading of the fwd prop. in the race of the fwd prop.}}\right\}$$

$$L_A^{(4N,\bar{n})}(\rho_A) = [\bar{K}'_{AA}(q_A = 4N)]^{-1}\left\{\left(\frac{\bar{W}_A^{(4N,\bar{m})}}{U}\right)_{t_F} - \sum_{\rho_F} L_F^{(0,\bar{n})}\bar{K}_{FA}^{(\bar{m},\bar{n})}(m_3=2N,\ q_A=4N)\right.$$

$$\left. + \left(\frac{\Delta\bar{W}_A}{U}\right)^{(4N,\bar{m})}_{\text{due to steady loading of the fwd prop. in the race of the fwd prop.}}\right\}$$

b) Complete interaction

1. $$L_F^{(0,\bar{n})}(\rho_F) = [\bar{K}'_{FF}(q_F=0)]^{-1}\left\{\left(\frac{\bar{W}_F^{(0,\bar{m})}}{U}\right)_{c+f} + \left(\frac{\bar{W}_F^{(0,\bar{m})}}{U}\right)_{t_A}\right.$$

$$- \sum_{\rho_A}\left[L_A^{(0,\bar{n})}\bar{K}_{AF}^{(\bar{m},\bar{n})}(m_2=0, q_F=0) + L_A^{(2N,\bar{n})}\bar{K}_{AF}^{(\bar{m},\bar{n})}(m_2=N, q_F=0)\right.$$

$$\left.\left. + L_A^{(4N,\bar{n})}\bar{K}_{AF}^{(\bar{m},\bar{n})}(m_2=2N, q_F=0)\right]\right\}$$

[Cont'd]

Table 1 (Cont'd)

2. $$L_F^{(2N,\bar{n})}(\rho_F) = [\bar{K}'_{FF}(q_F = -2N)]^{-1}\left\{\left(\frac{\bar{W}_F^{(2N,\bar{m})}}{U}\right)_{t_A} - \sum_{\rho_A}\left[L_A^{(0,\bar{n})}\bar{K}_{AF}^{(\bar{m},\bar{n})}(m_2=N, q_F=2N) + L_A^{(2N,\bar{n})}\bar{K}_{AF}^{(\bar{m},\bar{n})}(m_2=2N, q_F=2N) + L_A^{(4N,\bar{n})}\bar{K}_{AF}^{(\bar{m},\bar{n})}(m_2=3N, q_F=2N)\right]\right\}$$

3. $$L_F^{(4N,\bar{n})}(\rho_F) = [\bar{K}'_{FF}(q_F = -4N)]^{-1}\left\{\left(\frac{\bar{W}_F^{(4N,\bar{n})}}{U}\right)_{t_A} - \sum_{\rho_A}\left[L_A^{(0,\bar{n})}\bar{K}_{AF}^{(\bar{m},\bar{n})}(m_2=2N, q_F=4N) + L_A^{(2N,\bar{n})}\bar{K}_{AF}^{(\bar{m},\bar{n})}(m_2=3N, q_F=4N) + L_A^{(4N,\bar{n})}\bar{K}_{AF}^{(\bar{m},\bar{n})}(m_2=4N, q_F=4N)\right]\right\}$$

4. $$L_A^{(0,\bar{n})}(\rho_A) = [\bar{K}'_{AA}(q_A=0)]^{-1}\left\{\left(\frac{\bar{W}_A^{(0,\bar{m})}}{U}\right)_{c+f} + \left(\frac{\bar{W}_A^{(0,\bar{m})}}{U}\right)_{t_F} - \sum_{\rho_F}\left[L_F^{(0,\bar{n})}\bar{K}_{FA}^{(\bar{m},\bar{n})}(m_3=0, q_A=0) + L_F^{(2N,\bar{n})}\bar{K}_{FA}^{(\bar{m},\bar{n})}(m_3=N, q_A=0) + L_F^{(4N,\bar{n})}\bar{K}_{FA}^{(\bar{m},\bar{n})}(m_3=2N, q_A=0)\right] + \Delta\left(\frac{\bar{W}_A}{U}\right)^{(0,\bar{m})}_{\text{(due to steady and unsteady loadings of the forward propeller)}}\right\}$$

[Cont'd]

Table 1 (Cont'd)

$$5.\quad L_A^{(2N,\bar{n})}(\rho_A) = [\bar{K}'_{AA}(q_A=2N)]^{-1}\left\{\left(\frac{\bar{W}_A^{(2N,\bar{m})}}{U}\right)_{t_F}\right.$$

$$- \sum_{\rho_F}\left[L_F^{(0,\bar{n})}\bar{K}_{FA}^{(\bar{m},\bar{n})}(m_3=N, q_A=2N) + L_F^{(2N,n)}\bar{K}_{FA}^{(\bar{m},\bar{n})}(m_3=2N, q_A=2N)\right.$$

$$\left. + L_F^{(4N,\bar{n})}\bar{K}_{FA}^{(\bar{m},\bar{n})}(m_3=3N, q_A=2N)\right]$$

$$\left. + \Delta\left(\frac{\bar{W}_A}{U}\right)^{(2N,\bar{m})}_{\text{(due to steady and unsteady loadings of the forward propeller)}}\right\}$$

$$6.\quad L_A^{(4N,\bar{n})}(\rho_A) = [\bar{K}'_{AA}(q_A=4N)]^{-1}\left\{\left(\frac{\bar{W}_A^{(4N,\bar{m})}}{U}\right)_{t_F}\right.$$

$$- \sum_{\rho_F}\left[L_F^{(0,\bar{n})}\bar{K}_{FA}^{(\bar{m},\bar{n})}(m_3=2N, q_A=4N) + L_F^{(2N,\bar{n})}\bar{K}_{FA}^{(\bar{m},\bar{n})}(m_3=3N, q_A=4N)\right.$$

$$\left. + L_F^{(4N,\bar{n})}\bar{K}_{FA}^{(\bar{m},\bar{n})}(m=4N, q_A=4N)\right]$$

$$\left. + \Delta\left(\frac{\bar{W}_A}{U}\right)^{(4N,\bar{m})}_{\text{(due to steady and unsteady loadings of the forward propeller)}}\right\}$$

The above expressions for the interaction problem are now utilized for the final iterations. At this stage, two or three more iterations are sufficient to establish the final values of the steady and unsteady loadings and the corresponding thrust and torque.

TABLE 2

CASE $N_F \neq N_A$

PART A

1. Calculate inversion of self-induction kernels using $a_F = a_A = a_o = \frac{\pi}{J_s}$ where J_s is the advance coefficient of the system.

$$[\bar{K}_{FF}]^{-1} \quad (q_F = 0)$$

$$[\bar{K}_{FF}]^{-1} \quad (q_F = -2N_A)$$

$$[\bar{K}_{AA}]^{-1} \quad (q_A = 0)$$

$$[\bar{K}_{AA}]^{-1} \quad (q_A = 2N_F)$$

2. 0-iteration (first)

1) $$L_{F_0}^{(0,\bar{n})}(\rho_F) = [\bar{K}'_{FF}(q_F=0)]^{-1}\left\{\left(\frac{\bar{W}_F^{(0,\bar{m})}(r_F)}{U}\right)_{c+f+t_A}\right\}$$

2) $$L_{A_1}^{(0,\bar{n})}(\rho_A) = [\bar{K}'_{AA}(q_A=0)]^{-1}\left\{\left(\frac{\bar{W}_A^{(0,\bar{m})}(r_F)}{U}\right)_{c+f+t_F} - \sum_{\rho_F}\left[L_{F_0}^{(0,\bar{n})}\bar{K}_{FA}^{(\bar{m},\bar{n})}(m_3=0,q_A=0)\right] + \Delta\frac{\bar{W}_A^{(0,\bar{m})}}{U}\right\}$$

i-iteration:

1) $$L_{F_i}^{(0,\bar{n})}(\rho_F) = [\bar{K}'_{FF}(q_F=0)]^{-1}\left\{\left(\frac{\bar{W}_F^{(0,m)}(r_F)}{U}\right)_{c+f+t_A} - \sum_{\rho_A}\left[L_{A_i}^{(0,\bar{n})}\bar{K}_{AF}^{(\bar{m},\bar{n})}(m_2=0,q_F=0)\right]\right\}$$

2) $$L_{A_{i+1}}^{(0,\bar{n})}(\rho_A) = [\bar{K}'_{AA}(q_A=0)]^{-1}\left\{\left(\frac{\bar{W}_A^{(0,\bar{m})}(r_A)}{U}\right)_{c+f+t_F} - \sum_{\rho_F}\left[L_{F_i}^{(0,\bar{n})}\bar{K}_{FA}^{(\bar{m},\bar{n})}(m_3=0,q_A=0)\right]\right\}$$

[Cont'd]

Table 2 (Cont'd)

From the induced velocities, determine new a_F and a_A by utilizing Eq.(48) and then initiate an iterative procedure by recalculating the cross-coupling kernels K_{FA} and K_{AF} and $\frac{\Delta W_A}{U}$.

PART B

In the case $N_A \neq N_F$, Part B is made up of just section (b) of Table 1 since the steady state loadings only participate in the complete interaction problem.

1. $$L_{F_i}^{(0,\bar{n})}(\rho_F) = [\bar{K}'_{FF}(q_F=0)]^{-1}\left\{\left(\frac{\bar{W}_F^{(0,m)}(r_F)}{U}\right)_{c+f+t_A} - \sum_{\rho_A}\left[L_{A_i}^{(0,\bar{n})}\bar{K}_{AF}^{(\bar{m},\bar{n})}(m_2=0,q_A=0)\right]\right\}$$

2. $$L_{A_{i+1}}^{(0,\bar{n})}(\rho_A) = [\bar{K}'_{AA}(q_A=0)]^{-1}\left\{\left(\frac{\bar{W}_A^{(0,\bar{m})}(r_A)}{U}\right)_{c+f+t_F} + \Delta\frac{\bar{W}_A^{(0,\bar{m})}}{U} - \sum_{\rho_F}\left[L_{F_i}^{(0,\bar{n})}\bar{K}_{FA}^{(\bar{m},\bar{n})}(m_3=0,q_A=0)\right]\right\}$$

3. $$L_{F_{i+1}}^{(2N_A,\bar{n})}(\rho_F) = [\bar{K}'_{FF}(q_F=2N_A)]^{-1}\left\{\left(\frac{\bar{W}_F^{(2N_A,\bar{m})}}{U}\right)_{t_A} - \sum_{\rho_A}\left[L_{A_{i+1}}^{(0,\bar{n})}\bar{K}_{AF}^{(\bar{m},\bar{n})}(m_2=N_A,q_F=2N_A)\right]\right\}$$

4. $$L_{A_{i+2}}^{(2N_F,\bar{n})}(\rho_A) = [\bar{K}'_{AA}(q_A=2N_F)]^{-1}\left\{\left(\frac{\bar{W}_A^{(2N_F,\bar{m})}}{U}\right)_{t_F} + \Delta\frac{\bar{W}_A^{(2N_F,\bar{m})}}{U} - \sum_{\rho_F}\left[L_{F_i}^{(0,\bar{n})}\bar{K}_{FA}^{(\bar{m},\bar{n})}(m_3=N_F,q_A=2N_F)\right]\right\}$$

CORRELATION WITH EXPERIMENTS

To establish the accuracy and usefulness of the computational procedure, a correlation with existing experimental results has been made. Calculations have been performed for two CR configurations for which data are available from tests at the David W. Taylor Naval Ship Research and Development Center.[6,7] The data are for the two lowest frequencies, ℓ_i=0 and ℓ_i=1, and the computations have been limited to these frequencies.

The iterative procedure starts after all the required information has been computed and stored properly. The necessary kernel functions and inverse kernel functions are calculated for both a 4-0-4 and a 4-0-5 CR system for values of m and q as indicated in Tables 3 and 4.

TABLE 3

4-0-4 COUNTERROTATING SYSTEM

Matrix	Inverse Matrix	Values m	Values q	Matrix	Inverse Matrix	Values m	Values q
K_{AF}		0	0	K_{FA}		0	0
		4	0			4	0
		8	0			8	0
	K_{FF}		0		K_{AA}		0
K_{AF}		4	8	K_{FA}		4	8
		8	8			8	8
		12	8			12	8
	K_{FF}		-8		K_{AA}		8
K_{AF}		8	16	K_{FA}		8	16
		12	16			12	16
		16	16			16	16
	K_{FF}		-16		K_{AA}		16

TABLE 4

4-0-5 COUNTERROTATING SYSTEM

Matrix	Inverse Matrix	Values m	Values q	Matrix	Inverse Matrix	Values m	Values q
K_{AF}		0	0	K_{FA}		0	0
	K_{FF}		0		K_{AA}		0
K_{AF}		5	10	K_{FA}		N_F=4	$2N_F$=8
	K_{FF}		-10		K_{AA}		$2N_F$=8

Preliminary calculations have indicated that 4 to 5 iterations are sufficient for the part named "Auxiliary Calculations" whereas additional 2-3 iterations are required in the final stage of calculations (Part B) for both cases $N_F=N_A$ and $N_F\neq N_A$. The execution time for the iterative procedure, however, is minimal since the greatest time-consuming effort is that spent for the calculations of the inverse of the self-induction kernels $[K_{FF}]^{-1}$ and $[K_{AA}]^{-1}$ and these are performed only once, are stored in the tape files, and do not change from one iteration to the next.

The 4-0-4 CR system is composed of the David W. Taylor Naval Ship R&D Center Propeller 3686 forward and Propeller 3687-A aft, and the 4-0-5 set of Propeller 3686 forward and Propeller 3849 aft.[6,7] Propeller characteristics and flow conditions are given in Table 5.

TABLE 5

	Propeller 3686 Forward	Propeller 3687A Aft	Propeller 3849 Aft
Number of blades	4	4	5
EAR	0.303	0.322	0.379
P/D at 0.7R	1.291	1.320	1.287
Diameter, D , in	12.017	11.776	11.785
Rotation	LH*	RH*	RH*
n, rps	12	12	12
Speed, ft/sec	13.22	13.22	13.22
Advance ratio, J	1.1**	1.1**	1.1**

*LH rotation is ccw looking forward; RH rotation is cw looking forward.
**J is based on diameter of forward propeller #3686.

The axial clearance, ϵ , of both CR systems is set equal to 0.283 of the forward propeller radius r_{0F}.

Both systems were placed in uniform flow and run at a constant rotational speed of 12 rps. The water speed was varied so as to obtain values of advance coefficients between J=0.5 and approximately 1.4. A water speed of 13.22 ft/sec corresponds to the design advance coefficient J=1.1 . Design details of the 3 propellers, namely, pitch/diameter P/D, chord/diameter C/D, and thickness/chord t/c ratios are given in Table 6.

TABLE 6

DESIGN DETAILS OF MODEL PROPELLERS

r/r_oF	PROPELLER 3686			PROPELLER 3687A			PROPELLER 3849		
	P/D	C/D	t/c	P/D	C/D	t/c	P/D	C/D	t/c
0.2	1.426	0.1075	0.2214	1.289	0.1100	0.2161	1.169	0.1075	0.2214
0.3	1.396	0.1250	0.1688	1.291	0.1335	0.1581	1.207	0.1250	0.1688
0.4	1.366	0.1400	0.1321	1.295	0.1530	0.1203	1.243	0.1400	0.1321
0.5	1.336	0.1548	0.1027	1.302	0.1700	0.0935	1.277	0.1543	0.1027
0.6	1.310	0.1695	0.0785	1.311	0.1823	0.0727	1.288	0.1695	0.0784
0.7	1.291	0.1787	0.0604	1.326	0.1898	0.0569	1.287	0.1785	0.0604
0.8	1.278	0.1750	0.0463	1.344	0.1833	0.0442	1.293	0.1750	0.0463
0.9	1.269	0.1500	0.0367	1.361	0.1520	0.0362	1.321	0.1500	0.0367
.95	1.267	0.1220	0.0344	1.369	0.1220	0.0345	1.349	0.1220	0.0344

Results of calculations are given in Tables 7 to 9 for the 4-0-4 CR system and in Tables 10 and 11 for the 4-0-5 CR system.

Tables 7 and 10 show the results of the "Auxiliary Iterations" for both systems at the steady state flow conditions, compared with experiments.[6,7] The comparisons indicate excellent correlation.

Results of calculations for the time-dependent thrust and torque of the 4-0-4 CR system at 8 and 16 times the shaft frequency are presented in Table 8. Table 9 gives results for the potential and viscous flow conditions and for the combined effects. Experimental results are also included in the table for comparison. The correlation has improved considerably over the results of Reference [4] although it may merely be considered as ranging

from satisfactory to good. It must be kept in mind that the viscous effects are determined approximately.

Results of the theoretical calculations for the 4-0-5 CR system are presented in Table 10 for the "Auxiliary Iterations" at the steady state flow conditions, showing that four iterations are sufficient for convergence of the results to their final values. The correlation between theory and experiments is considered very good.

Table 11 gives the results of the potential and viscous flow calculations separately and combined. The thrust and torque coefficients at steady state flow conditions, and the unsteady horizontal and vertical force and moment coefficients at nine times the shaft frequency are calculated for the potential flow for both units of the CR system. For the after propeller, which operates in the wake of the forward propeller, calculations were made under viscous flow conditions at nine times the shaft frequency.

Table 12 shows more clearly the comparison between calculated and measured values for both CR systems. Considering that no measurements of the wake of the forward propeller were made and the viscosity effects were determined approximately, the calculated amplitude of the forces and moments may be characterized as satisfactory. The error may also lie in the experimental results. As Reference [7] reports, one possible cause of the difference between experiment and theory is that the somewhat bulky dynamometer was downstream of the propellers when the after propeller forces were measured and upstream for the forward propeller measurements. As for the phases, Reference [7] also reported inability to obtain good average values because the phase variations were too great.

Reference [21] reports the results of the latest experimental investigation of the same CR systems, which repeated the tests in uniform flow and conducted additional tests in a 4-cycle wake, using the same procedure. The uniform flow results reported in References [7] and [21] are given in Table 13 together with the theoretically calculated results, showing inconsistencies in the phases of the two experiments and the spread in amplitudes, up to 10% for the 4-0-4 system, but as much as a factor of five in the values of forward propeller bending moment at nine times the shaft frequency for the 4-0-5 system for no apparent reason.

Table 14 shows the differences in amplitude and phase between each of the experiments and the calculations. It is appreciated that a degree of difficulty is involved in the measurement of forces and moments exerted on each component of the CR system. Therefore, the experimental results should not be considered as final and the existing differences between theory and experiment must be examined cautiously. Reference [21] recommends that for future experiments the shafts be locked together mechanically and that a second dynamometer be used so that unsteady measurements can be made on both propellers simultaneously to insure that conditions are the same for both propellers.

At any rate, it appears that inclusion of the potential and viscous effects of the forward propeller on the after, together with some refinements of the numerical procedure, have brought the theoretical results into better agreement with experimental than was the case in Reference [4]. Particularly in the case of the 4-0-5 system, the vibratory side forces and moments of the forward propeller are shown theoretically to be higher than those of the after propeller, which the experiments have consistently shown although this was difficult to understand physically.

The present analyses can be applied if and when wake measurements are made in the plane of the aft propeller with the forward propeller in place, thus providing a more accurate determination of the effect of the forward propeller race on the potential and viscous flows to the after propeller. The analysis and coding can be extended also for nonuniform inflow conditions due to hull wake.

TABLE 7

4-0-4 COUNTERROTATING PROPELLER

FWD 3686 L.H.; AFT 3687A R.H.

AUXILIARY ITERATIONS

ITEMS		ITERATION 1	2	3	4	5	EXPERIMENTS
a_F		2.856	2.667	2.725	2.699	2.707	
a_A		2.856	2.559	2.669	2.633	2.647	
$\bar{K}_T^F$	Re	- .1595	- .1153	- .1277	- .1219	- .1237	
	Amp.	.1595	.1153	.1277	.1219	.1237	.125
	Phase	180°	180°	180°	180°	180°	
$\bar{K}_Q^F$	Re	.0332	.0239	.0265	.0253	.0257	
	Amp.	.0332	.0239	.0265	.0253	.0257	.0315
	Phase	0°	0°	0°	0°	0°	
$\bar{K}_T^A$	Re	- .180	- .1319	- .1539	- .1469	-.1496	
	Amp.	.180	.1319	.1539	.1496	.1496	.150
	Phase	180°	180°	180°	180°	180°	
$\bar{K}_Q^A$	Re	.0376	.0275	.0320	.0306	.0315	
	Amp.	.0376	.0275	.0320	.0306	.0315	.0315
	Phase	0°	0°	0°	0°	0°	

Inflow field is calculated with a_F = 98% a_o = 2.799

and a_A = 102% a_o = 2.913

TABLE 8

4-0-4 COUNTERROTATING PROPELLER

FWD 3686 L.H.; AFT 3687A R.H.

FINAL ITERATIONS

FREQ	ITEMS	ITERATION #1 RE	IM	AMP	PHASE	ITERATION #2 RE	IM	AMP	PHASE	EXPER. AMP
Q=0	$\tilde{K}_T^F$	-.12305	0	.1231	180°	-.1227	.00066	.1227	179.7°	.125
	$\tilde{K}_Q^F$	.02558	0	.0255	180°	.02552	-.00014	.0255	-.31°	.0315
	$\tilde{K}_T^A$	-.14912	0	.1491	180°	-.15219	.00126	.152	179.5°	.150
	$\tilde{K}_Q^A$	.03106	0	.0311	180°	.03170	-.00026	.0317	-.47°	.0315
Q=8	$\tilde{K}_T^F$	.01528	.00551	.0162	19.8°	.01551	.00565	.0165	20°	.0285
	$\tilde{K}_Q^F$	-.00319	-.00115	.0034	-160.2°	-.00324	-.00118	.0034	-160°	.0058
	$\tilde{K}_T^A$	.01006	-.01619	.0191	-58.2°	.00968	-.01721	.0197	-60.6°	.0095
	$\tilde{K}_Q^A$	-.00208	.00337	.0039	121.6°	-.0020	.00358	.0041	119.2°	.0022
Q=16	$\tilde{K}_T^F$	.00796	-.00126	.0081	-8.99°	.00805	-.00121	.0081	-8.5°	.0180
	$\tilde{K}_Q^F$	-.00165	.00026	.0016	171.3°	-.00167	.00025	.0016	171.5°	.0047
	$\tilde{K}_T^A$	-.00618	.00275	.0067	156°	-.00617	.00271	.0067	156.2°	.0080
	$\tilde{K}_Q^A$	.00129	-.00058	.0014	-24.1°	.00128	-.00057	.0014	-23.9°	.0020

TABLE 9

4-0-4 COUNTERROTATING PROPELLER

FWD 3686 L.H.

AFT 3687A R.H.

COMBINED POTENTIAL AND VISCOUS EFFECTS

		POTENTIAL			VISCOUS			COMBINED EFFECTS				
FREQ	ITEMS	RE	IM	AMP	RE	IM	AMP	RE	IM	AMP	PHASE	EXPER AMP
Q=0	$\bar{K}_T^F$	-.1227	.00066	.1227						.123	180°	.125
	$\bar{K}_Q^F$	.0255	-.00014	.0255						.026	.3°	.0315
	$\bar{K}_T^A$	-.1522	.00126	.152						.152	180°	.150
	$\bar{K}_Q^A$	.03170	-.00026	.0317						.032	-.5°	.0315
Q=8	$\tilde{K}_T^F$	.01551	.00565	.0165						.017	28°	.0285
	$\tilde{K}_Q^F$	-.00324	-.00118	.0034						.003	-160°	.0058
	$\tilde{K}_T^A$	.00968	-.01721	.0197	.00171	.0088	.00898	.01138	-.00838	.014	-36°	.0095
	$\tilde{K}_Q^A$	-.0020	.00358	.0041	-.00036	-.00183	.00186	-.00236	.00175	.0029	143°	.0022
Q=16	$\tilde{K}_T^F$	.00805	-.00121	.0081						.0081	-9°	.0180
	$\tilde{K}_Q^F$	-.00167	.00025	.0016						.0016	172°	.0047
	$\tilde{K}_T^A$	-.00617	.00271	.0067	.00583	.00038	.00584	-.00034	.0031	.0031	96°	.0080
	$\tilde{K}_Q^A$	.00128	-.00057	.0014	-.00121	-.00007	.00121	.00007	-.00064	.0006	-83°	.0020

TABLE 10

4-0-5 COUNTERROTATING PROPELLER

FWD 3686 L.H. 4-Bladed

AFT 3849 R.H. 5-Bladed

AUXILIARY ITERATIONS

ITEMS		ITERATION 1	2	3	4	EXPER
a_F		2.856	2.856	2.756	2.729	
a_A		2.856	2.579	2.629	2.635	
$\overline{K}_T^F$	Re	- .1483	- .1364	- .1297	- .1298	
	Amp	.1483	.1364	.1297	.1297	.130
	Phase	180°	180°	180°	180°	
$\overline{K}_Q^F$	Re	.0308	.0283	.0269	.0270	
	Amp	.0308	.0283	.0269	.0270	.030
	Phase	0°	0°	0°	0°	
$\overline{K}_T^A$	Re	- .1049	- .1324	- .1323	- .1322	
	Amp	.1049	.1324	.1323	.1322	.130
	Phase	180°	180°	180°	180°	
$\overline{K}_Q^A$	Re	.0212	.0268	.0268	.0267	
	Amp	.0212	.0268	.0267	.0267	.028
	Phase	0°	0°	0°	0°	

The inflow field is calculated with a_F = 96.5% a_o = 2.756
and $a_A = a_o$ = 2.856

TABLE 11

4-0-5 COUNTERROTATING PROPELLER

FWD 3686 L.H. 4-Bladed

AFT 3849 R.H. 5-Bladed

POTENTIAL AND VISCOUS EFFECTS

FREQ	ITEMS	POTENTIAL				VISCOUS				COMBINED EFFECTS				EXPER AMP
		RE	IM	AMP	PHASE	RE	IM	AMP	PHASE	RE	IM	AMP	PHASE	
Q=0	$\tilde{K}_T^F$	-.1298		.1298	180°							.130		.130
	$\tilde{K}_Q^F$	.0270		.027	0°							.027		.03
	$\tilde{K}_T^A$	-.1322		.1322	180°							.132		.130
	$\tilde{K}_Q^A$	.0267		.0267	0°							.027		.028
Q=9	$\tilde{K}_{FH}^F$	.00536	.00319	.0062	30.8°							.0062	31°	.0075
	$\tilde{K}_{QH}^F$	.00260	.00172	.0031	33.5°							.0031	34°	.0040
	$\tilde{K}_{FH}^A$	.00504	-.00705	.0087	-54°	.00033	.00387	.0039	85.1°	.00537	-.00318	.0062	-30.6°	.0057
	$\tilde{K}_{QH}^A$	.00255	-.00396	.0047	-57.2°	.00036	.00184	.0019	78.9°	.00291	-.00212	.0036	-36.1°	.0023
	$\tilde{K}_{FV}^F$	.00319	-.00536	.0062	-59.2°							.0062	-59°	.0074
	$\tilde{K}_{QV}^F$	.00172	-.0026	.0031	-56.5°							.0031	-56°	.0041
	$\tilde{K}_{FV}^A$	.00705	.00504	.0087	35.6°	-.00387	.00033	.0039	175°	.00318	.00537	.0062	59.4°	.0046
	$\tilde{K}_{QV}^A$	.00396	.00255	.0047	32.8°	-.00184	.00036	.0019	168.9°	.00212	.00291	.0036	53.9°	.0023

TABLE 12

CORRELATION OF THEORETICAL CALCULATIONS WITH RESULTS OF EXPERIMENTS

4-0-4 CR SYSTEM

FREQ	ITEMS	CALCULATIONS AMP	CALCULATIONS PHASE	EXPERIMENTS AMP	EXPERIMENTS PHASE	CALC. AMP. / EXP. AMP.	CALC. PHASE MINUS EXP. PHASE
Q=0	$\bar{K}_T^F$	.123	180°	.125		.984	
	$\bar{K}_Q^F$	.026	.3°	.0315		.826	
	$\bar{K}_T^A$	.152	180°	.150		1.01	
	$\bar{K}_Q^A$	.032	-.5°	.0315		1.01	
Q=8	$\tilde{K}_T^F$	.017	28°	.0285	-136°	.596	164°
	$\tilde{K}_Q^F$	.003	-160°	.0058	-152°	.517	-8°
	$\tilde{K}_T^A$	.014	-36°	.0095	-80°	1.47	49°
	$\tilde{K}_Q^A$	.0029	143°	.0022	-260°	1.32	43°
Q=16	$\tilde{K}_T^F$	.0081	-9°	.0180	-30°	.450	21°
	$\tilde{K}_Q^F$	.0016	172°	.0047	-45°	.340	217°
	$\tilde{K}_T^A$	.0031	96°	.0080	80°	.388	16°
	$\tilde{K}_Q^A$	.0006	83°	.0020	-103°	.300	186°

4-0-5 CR SYSTEM

FREQ	ITEMS	CALCULATIONS AMP	CALCULATIONS PHASE	EXPERIMENTS AMP	EXPERIMENTS PHASE	CALC. AMP. / EXP. AMP.	CALC. PHASE MINUS EXP. PHASE
Q=0	$\bar{K}_T^F$	.130	180°	.130		1.00	
	$\bar{K}_Q^F$	.027	0°	.030		.90	
	$\bar{K}_T^A$	.132	180°	.130		1.01	
	$\bar{K}_Q^A$	.027	0°	.028		.964	
Q=9	$\tilde{K}_{FH}^F$	.0062	31°	.0075	210°	.827	-179°
	$\tilde{K}_{QH}^F$	.0031	34°	.0040	-45°	.775	79°
	$\tilde{K}_{FH}^A$	.0062	-30.6°	.0057	123°	1.09	-154°
	$\tilde{K}_{QH}^A$	.0036	-36.1°	.0023	-2°	1.56	-34°
	$\tilde{K}_{FV}^F$	.0062	-59°	.0074	120°	.836	-179°
	$\tilde{K}_{QV}^F$	.0031	-56°	.0041	47°	.756	-103°
	$\tilde{K}_{FV}^A$	.0062	59.4°	.0046	30°	1.35	29°
	$\tilde{K}_{QV}^A$	.0036	53.9°	.0023	97°	1.56	-43°

TABLE 13

RESULTS OF EXPERIMENTAL MEASUREMENTS OF REFS. [7] AND [21] IN UNIFORM FLOW COMPARED WITH CALCULATIONS BY THE PRESENT THEORY

FREQ	ITEMS	CALCULATIONS AMP	CALCULATIONS PHASE	EXPERIMENTS REF.[7] AMP	EXPERIMENTS REF.[7] PHASE	EXPERIMENTS REF.[21] AMP	EXPERIMENTS REF.[21] PHASE	REF. 7 AMP / REF.21 AMP
4-0-4 CR SYSTEM								
Q=8	$\tilde{K}_T^F$	.017	28°	.0285	-136°	.0270	-153°	1.05
	$\tilde{K}_Q^F$	.0030	-160°	.0058	-152°	.0055	-168°	1.05
	$\tilde{K}_T^A$	.014	-36°	.0095	- 80°	.0095	-134°	1.00
	$\tilde{K}_Q^A$	.0029	143°	.0022	-260° / +100°	.0020	-147°	1.10
4-0-5 CR SYSTEM								
Q=9	$\tilde{K}_{FH}^F$	.0062	31°	.0075	210°	.0059	215°	1.27
	$\tilde{K}_{QH}^F$	.0031	34°	.0040	-45°	.0198	-37°	0.20
	$\tilde{K}_{FH}^A$	.0062	-31°	.0057	123°	.0047	-50°	1.21
	$\tilde{K}_{QH}^A$	.0036	-36°	.0023	-2°	.0020	-	1.15
	$\tilde{K}_{FV}^F$	.0062	-59°	.0074	120°	.0073	140°	1.01
	$\tilde{K}_{QV}^F$	.0031	-56°	.0041	47°	.0203	47°	0.20
	$\tilde{K}_{FV}^A$	.0062	59°	.0046	30°	.0042	-39°	1.10
	$\tilde{K}_{QV}^A$	.0036	54°	.0023	97°	.0018	-	1.27

TABLE 14

COMPARISON OF EXPERIMENTAL RESULTS OF REFS. [7] AND [21] WITH THEORETICAL RESULTS

FREQ	ITEMS	REFERENCE [7] CALC. AMP / EXP.[7] AMP	REFERENCE [7] CALC. PHASE MINUS EXP.[7] PHASE	REFERENCE [21] CALC. AMP / EXP.[21] AMP	REFERENCE [21] CALC. PHASE MINUS EXP.[21] PHASE
4-0-4 CR SYSTEM					
Q=8	$\tilde{K}^F_T$	0.60	164°	0.63	181°
	$\tilde{K}^F_Q$	0.52	-8°	0.54	8°
	$\tilde{K}^A_T$	1.47	44°	1.47	98°
	$\tilde{K}^A_Q$	1.32	43°	1.45	-70°
4-0-5 CR SYSTEM					
Q=9	$\tilde{K}^F_{FH}$	0.83	-179°	1.05	-184°
	$\tilde{K}^F_{QH}$	0.77	79°	0.16	71°
	$\tilde{K}^A_{FH}$	1.09	-154°	1.32	19°
	$\tilde{K}^A_{QH}$	1.56	-34°	1.80	-
	$\tilde{K}^F_{F_V}$	0.84	-179°	0.85	-199°
	$\tilde{K}^F_{QV}$	0.76	-103°	0.15	-103°
	$\tilde{K}^A_{FV}$	1.35	29°	1.47	98°
	$\tilde{K}^A_{QV}$	1.56	-43°	2.00	-

SUMMARY AND CONCLUSIONS

Linearized unsteady lifting-surface theory has been applied in the study of two interacting propellers of a counterrotating system, when both units operate in a spatially non-uniform inflow. A mathematical model is introduced taking into account the exact geometry of the propulsive system as well as the three-dimensional spatially varying inflow. The propeller blades are considered to be of finite thickness and lying on a helicoidal surface of varying pitch. The blades have arbitrary planform, camber and sweep angle. The flow conditions have been taken as realistically as possible by considering the fact that the after propeller operates in the race of the forward propeller so that potential and viscous effects of the wake are incorporated in the analysis and program.

The computational procedure, however, has been developed and adapted to the CDC 6600 and 7600, or Cyber 176, high-speed digital computer, for the case where both units operate with the same RPM in a uniform inflow field.

The uniformity of the inflow field provides for a better understanding of the mechanism of interaction of the CR system since the presence of wake harmonics would have such a dominant effect as to mask the interaction phenomenon.

The study provides information about the steady and unsteady blade loading distributions and the corresponding hydrodynamic forces and moments on both components of the propulsive device.

Rules have been established for the presence or absence of the steady and unsteady hydrodynamic forces and moments when the CR system is made up of equal and unequal numbers of blades. In fact, when the propellers of the CR system have equal number of blades only the steady and unsteady thrust and torque will be generated on each propeller of the CR system, at zero and blade-blade crossing frequencies or multiples thereof ($q=2\ell N$, $\ell=1,2,3,$ ... and N = common number of blades). When the CR system is made up of propellers with unequal number of blades, i.e., $N_F \neq N_A$, then steady thrust and torque will be generated and unsteady side forces and moments will be present at frequency order $q=2\ell N_F+1$ or $q=2\ell N_A-1$.

From a limited number of calculations, the correlation with experiment varies from very good to satisfactory. The steady-state calculated thrust and torque compare very well with experimental values; for the unsteady flow condition, the correlation can be classified as satisfactory to good. The results for 4-0-5 CR system show better agreement than those for the 4-0-4 CR system.

The additional effects of the forward propeller race on the after propeller, due to potential and viscous flow conditions, play an important role in determining the unsteady loading of the after propeller. This, coupled with the fact that more refined numerical methods have been used in the potential part of the interaction problem, has brought the final results into better agreement with experiment than those reported in Reference [4].

The viscous contribution, a decisive factor, has been calculated by an approximate method,[16] and hence there is still room for improvement. By measuring the wake in the plane of the after propeller with the forward propeller in place, a more accurate determination can be made of the effect of the forward propeller race on the potential as well as the viscous flow to the after propeller. Of course, the error may also lie with the experimentation. As reported in References [7] and [21], one possible source of error is that the dynamometer was downstream of the propellers when the after propeller forces were measured and upstream for the forward propeller measurements. Also, phase variations were too great for good average values to be obtained in the measurements.

Because of the existing differences between the two sets of experimental measurements, both taken by the same procedure but at a different time (a year apart), the measured values cannot be considered as final and therefore the existing differences between experiment and theory should be examined cautiously.

It can be stated that inclusion of the correct race and viscous effects of the forward propeller has brought the calculations into much better agreement with measurements. Indeed, in some cases the vibratory hydrodynamic forces of the forward propeller are larger in magnitude than those of the after propeller, a fact which was shown in all the experiments.

It is highly important to note that for the 4-0-4 set, the magnitudes of the measured and calculated vibratory thrust and torque of both the forward and after propellers at the passage frequencies of 8 times shaft rate are large in relation to the mean values. They are large in respect to the experience gained in calculating the amplitudes at blade rate for single propellers abaft merchant hulls.

For the 4-0-5 system, the vibratory side forces and moments also appear large relative to single propeller experience but not as large as in the 4-0-4 system. This indicates that increased spacing of the propellers should be examined by systematic calculations to determine those spacings at which these mutually induced vibratory forces can be ameliorated. Otherwise both the experimental and the calculated results indicate that systems of counterrotating propellers may have highly objectionable excitations.

The present analysis and basic program can be extended for nonuniform inflow conditions due to hull wake, and also can be used as a nucleus for the analysis for another propulsion system such as a ducted propeller,[18] or a pump-jet configuration.[19]

The developed programs require approximately 15-20 minutes execution time on the CDC 6600 for each configuration, performing the required iterations, calculating the steady and unsteady loadings and resulting hydrodynamic forces and moments on each member of a set due to potential and viscous effects, and computing the corresponding blade pressure distributions on each propeller.

REFERENCES

1. Hadler, J.B., Morgan, W.B., and Meyers, K.A., "Advanced Propeller Propulsion for High-Powered Single-Screw Ships," Transactions,SNAME, Vol.72, 1964.

2. Wereldsma, R., "Investigations on the Vibratory Output of Contra-rotating Screw Propellers," 7th Symposium on Naval Hydrodynamics, Rome, August 25-30, 1968.

3. Tsakonas, S. and Jacobs, W.R., "Counterrotating and Tandem Propellers Operating in Spatially Varying, Three-Dimensional Flow Fields, Part I — Analysis," Davidson Laboratory Report 1335, Stevens Institute of Technology, September 1968.

4. Tsakonas, S., Jacobs, W.R., and Ali, M., "Steady and Unsteady Loadings and Hydrodynamic Forces on Counterrotating Propellers," Davidson Laboratory Report SIT-DL-76-1899, July 1976.

5. Jacobs, W.R. and Tsakonas, S., "A New Procedure for the Solution of Lifting Surface Problems," J. Hydronautics, Vol.3, No.1, January 1969.

6. Hecker, R. and McDonald, N.A., "The Effect of Axial Spacing and Diameter on the Powering Performance of Counterrotating Propellers," David Taylor Model Basin Report 1342, February 1960.

7. Miller, M.L., "Experimental Determination of Unsteady Forces on Counter-rotating Propellers in Uniform Flow," David W. Taylor Naval Ship Research and Development Center Report SPD-659-01, May 1976.

8. Tsakonas, S., Jacobs, W.R., and Ali, M.R., "Propeller Blade Pressure Distribution Due to Loading and Thickness Effects," Report SIT-DL-76-1869, Stevens Institute of Technology, April 1976; J. Ship Research, Vol.23, No.2, June 1979.

9. Tsakonas, S., Jacobs, W.R., and Ali, M.R., "Documentation of a Computer Program for the Pressure Distribution, Forces and Moments on Ship Propellers in Hull Wakes," Report SIT-DL-76-1863, Stevens Institute of Technology, 1976 (in 4 volumes).

10. Tsakonas, S. and Jacobs, W.R., "Propeller Loading Distributions," DL Report 1319, Stevens Institute of Technology, August 1968; J. Ship Research, Vol.13, No.4, December 1969.

11. Jacobs, W.R. and Tsakonas, S., "Propeller Induced Velocity Field Due to Thickness and Loading Effects," Report SIT-DL-73-1681, Stevens Institute of Technology, July 1973.

12. Jacobs, W.R., Mercier, J., and Tsakonas, S., "Theory and Measurements of the Propeller-Induced Vibratory Pressure Field," Report SIT-DL-70-1485, Stevens Institute of Technology, December 1970; J. Ship Research, Vol.16, No.2, June 1972.

13. Tsakonas, S., Breslin, J.P., and Miller, M., "Correlation and Application of an Unsteady Flow Theory for Propeller Forces," Transactions, SNAME, Vol.75, 1967.

14. Strasberg, M. and Breslin, J.P., "The Frequencies of the Alternating Forces Due to Interactions of Contrarotating Propellers," J. Hydronautics, April 1976.

15. Tsakonas, S., Breslin, J.P., and Jacobs, W.R., "Blade Pressure Distribution for a Moderately Loaded Propeller," Report SIT-DL-80-9-2063, Stevens Institute of Technology, September 1980.

16. Kemp, N.H. and Sears, W.R., "The Unsteady Forces Due to Viscous Wakes in Turbomachines," J. of Aeronautical Sciences, Vol.22, No.7, July 1955.

17. Silverstein, A., Katzoff, S., and Bullivant, W.K., "Downwash and Wake Behind Plain and Flapped Airfoils," NACA Report 651, 1939.

18. Tsakonas, S., Jacobs, W.R., and Ali, M.R., "Propeller-Duct Interaction Due to Loading and Thickness Effects," Report SIT-DL-75-1722, Stevens Inst. of Technology, April 1975, presented at the "Propeller '78" Symposium, Virginia Beach, Virginia, May 1978.

19. Jacobs, W.R., Tsakonas, S., and Liao, Ping, "Linearized Unsteady Lifting Surface Theory Applied to the Pump-Jet Propulsion System," Technical Report SIT-DL-80-9-2173, Stevens Institute of Technology, August 1981.

20. Hoerner, S.F., Fluid-Dynamic Drag, published by the author, 1965.

21. Miller, M.L., "Experimental Determination of Unsteady Forces on Contrarotating Propellers for Application to Torpedoes," David W. Taylor Naval Ship Research and Development Center Report SPD-659-02, December 1981.

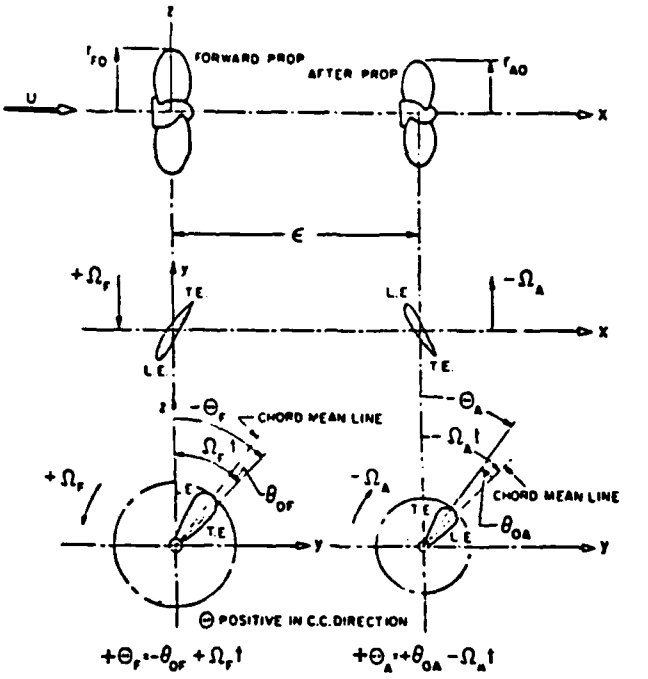

Fig. 1: Counterrotating propeller arrangement – angular coordinates.

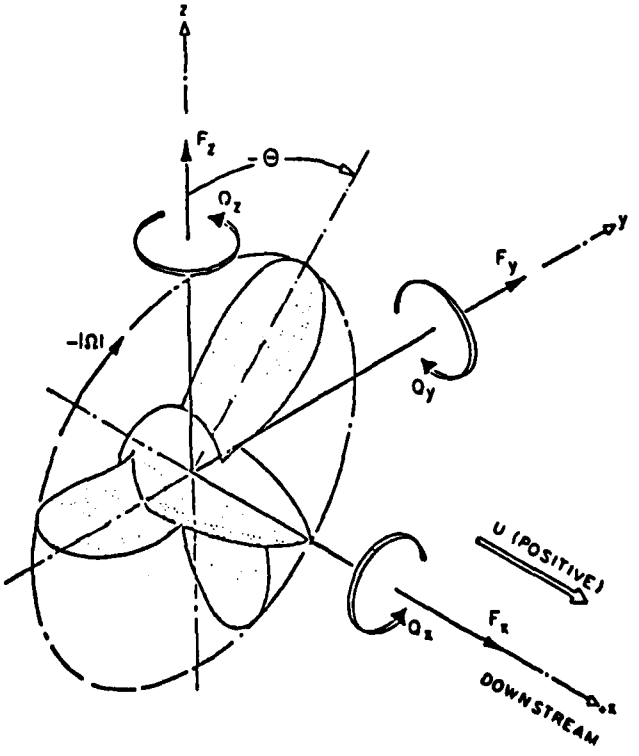

Fig. 2: Resolution of forces and moments.

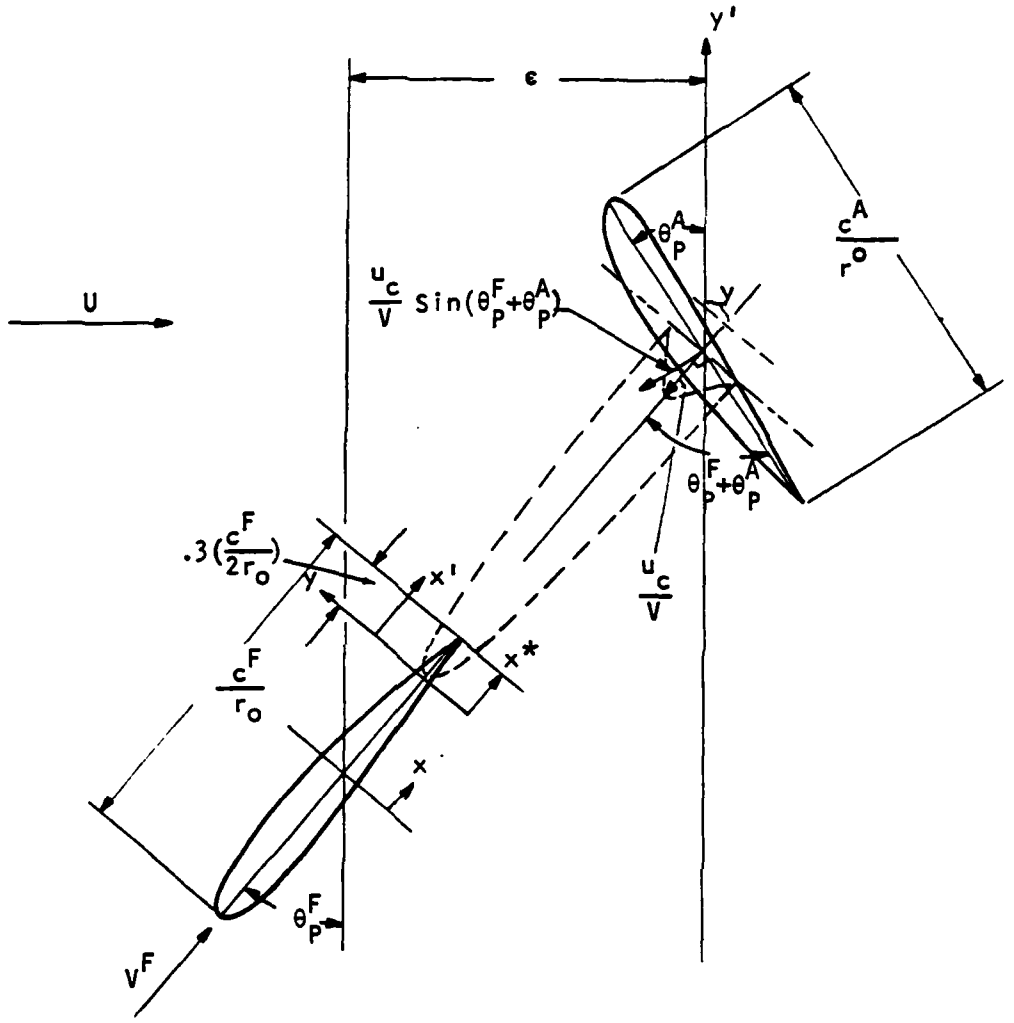

Fig. 3: Expanded view of two propeller blades at a particular radial position, r_F.

APPENDIX A

RACE EFFECT ON THE AFTER PROPELLER

In the course of a re-examination of the theoretical development of Reference 4, it was found that the behavior of the velocity field for points inside the propeller race is quite different from that at any other point in the field around an operating propeller. The existing theory and program dealing with the propeller-induced velocity field have therefore been modified to include the region of the propeller race in which the after propeller operates. *This additional wake effect,* designated by* $\Delta W_A/U$, *has been developed and incorporated in the program as "Correction Term."* Thus, the exact wake-velocity field is determined in which the after propeller operates.

The W_A induced velocity at points on the right-handed after propeller by the presence of a left-handed forward propeller is given by

$$W_A(x_A,r_A,\varphi_A,t) = -\frac{1}{4\pi\rho_f U}\sum_{n=1}^{N_F}\int_{\xi_F}\int_{\rho_F}\sum_{\lambda=0}\Delta p_F^{(\lambda)}(\xi_F,\rho_F,\theta_F)e^{-i\lambda\Omega_F t}$$

$$\cdot\frac{\partial}{\partial n_A'}\int_{-\infty}^{x_A} e^{-i\lambda[a_F(\tau'-x_A)-\bar{\theta}_{Fn}]}\left(a_F\frac{\partial}{d\xi_F}-\frac{1}{\rho_F^2}\frac{\partial}{\partial\theta_{OF}}\right)\left(\frac{1}{R_{FA}}\right)\rho_F d\rho_F d\xi_F d\tau' \qquad (A\text{-}1)$$

where

$$\frac{\partial}{\partial n_A'} = \frac{r_A}{\sqrt{1+a_A^2 r_A^2}}\left(a_A\frac{\partial}{\partial x_A}-\frac{1}{r_A^2}\frac{\partial}{\partial\varphi_{OA}}\right)$$

since

$$x_A = \frac{\varphi_{OA}}{a_A}+\epsilon \quad \text{and} \quad \frac{\partial}{\partial\varphi_{OA}} = \frac{1}{a_A}\frac{\partial}{\partial x_A}$$

$$\frac{\partial}{\partial n_A'} = \frac{1}{\sqrt{1+a_A^2 r_A^2}}\left(a_A r_A-\frac{1}{a_A r_A}\right)\frac{\partial}{\partial x_A}$$

In (A-1), $R_{FA}=\left\{(\tau'-\xi_F)^2+r_A^2+\rho_F^2-2r_A\rho_F\cos\left[\theta_{OF}+\varphi_{OA}-(\Omega_F+\Omega_A)t+\bar{\theta}_{Fn}-a_F(\tau'-x_A')\right]\right\}^{\frac{1}{2}}$

*As devised by Drs. J.P. Breslin and T.R. Goodman.

In the equal RPM case: $|\Omega_A| = (\Omega_F) = \Omega$, $a_A = a_F = a$

and with $-\Omega t = +\Theta$, $-(\Omega_F+\Omega_A)t = +2\Theta$.

Let $\tau' - x_A = \tau$, $d\tau' = d\tau$

$$I_\tau = \int_{-\infty}^{o} e^{-i\lambda[a_F\tau-\bar{\theta}_{Fn}]}\left(a_F\frac{\partial}{\partial\xi_F} - \frac{1}{\rho_F^2}\frac{\partial}{\partial\theta_{0F}}\right)\left(\frac{1}{R_{FA}}\right)\rho_F d\rho_F d\xi_F d\tau$$

where

$$R_{FA} = \left\{(\tau+x_A-\xi_F)^2 + r_A^2+\rho_F^2-2r_A\rho_F\cos[\theta_{0F}+\varphi_{0A}+2\Theta+\bar{\theta}_{Fn}-a_F\tau]\right\}^{\frac{1}{2}}$$

Then

$$\frac{\partial I_\tau}{\partial x_A} = \int_{-\infty}^{o} e^{-i\lambda(a_F\tau-\bar{\theta}_{Fn})}\left(a_F\frac{\partial^2}{\partial x_A\partial\xi_F} - \frac{1}{\rho_F^2}\frac{\partial^2}{\partial x_A\partial\theta_{0F}}\right)\left(\frac{1}{R_{FA}}\right)\rho_F d\rho_F d\xi_F d\tau$$

But $$\frac{\partial^2}{\partial x_A\partial\xi_F} = -\frac{\partial^2}{\partial x_A^2}$$

Therefore

$$\frac{\partial I_\tau}{\partial x_A} = -\int_{-\infty}^{o} e^{-i\lambda(a_F\tau-\bar{\theta}_{Fn})}\left(a_F\frac{\partial^2}{\partial x_A^2} + \frac{1}{\rho_F^2}\frac{\partial^2}{\partial x_A\partial\theta_{0F}}\right)\left(\frac{1}{R_{FA}}\right)\rho_F d\rho_F d\xi_F d\tau \qquad (A\text{-}2)$$

Furthermore for points inside the propeller race, Laplace's equation written in cylindrical coordinates takes the form

$$\frac{\partial^2}{\partial x_A^2}\left(\frac{1}{R}\right) + \frac{1}{\rho}\frac{\partial}{\partial\rho}\left(\rho\frac{\partial}{\partial\rho}\frac{1}{R}\right) + \frac{1}{\rho^2}\frac{\partial^2}{\partial\theta_o^2}\left(\frac{1}{R}\right) = -\frac{4\pi}{\rho_F}\delta(\tau+x_A-\xi_F)\delta(r_A-\rho_F)$$
$$\delta(\theta_{0F}+\varphi_{0A}+2\Theta+\bar{\theta}_{Fn}-a_F\tau) .$$

Thus whenever the field point coincides with the helices of the wake,

$$\frac{\partial^2}{\partial x_A^2}\left(\frac{1}{R}\right) = -\frac{4\pi}{\rho_F}\delta(\tau+x_A-\xi_F)\delta(r_A-\rho_F)\delta(\theta_{0F}+\varphi_{0A}+2\Theta+\bar{\theta}_{Fn}-a_F\tau) - \left[\frac{1}{\rho_F}\frac{\partial}{\partial\rho_F}\left(\rho_F\frac{\partial}{\partial\rho_F}\right)\left(\frac{1}{R}\right)\right.$$
$$\left. + \frac{1}{\rho_F^2}\frac{\partial^2}{\partial\theta_{0F}^2}\left(\frac{1}{R}\right)\right] \qquad (A\text{-}3)$$

The induction ΔW_A is the first term of $\frac{\partial^2}{\partial x_A^2}\left(\frac{1}{R}\right)$

$$\Delta W_A^{(1)} = -\frac{1}{4\pi\rho_f U}\frac{1}{\sqrt{1+a_A^2 r_A^2}}\left(a_A r_A - \frac{1}{a_A r_A}\right)$$

$$\cdot \sum_{n=1}^{N_F}\left\{\int_\xi\int_\rho \sum_{\lambda=0} \Delta p_F^{(\lambda)}(\xi,\rho,\theta)e^{i\lambda\Theta}\int_{-\infty}^{o} e^{-i\lambda(a_F\tau-\bar\theta_{Fn})}\rho_F d\rho_F d\xi_F\right.$$

$$\left.\cdot\frac{4\pi a_F}{\rho_F}\delta(\tau+x_A-\xi_F)\delta(r_A-\rho_F)\delta(\theta_{0F}+\varphi_{0A}+2\Theta+\bar\theta_{Fn}-a_F\tau)\,d\tau\right\} \qquad (A\text{-}4)$$

$$\{\} = \int_\xi \sum_{\lambda=0} \Delta p_F^{(\lambda)}(\xi_F, r_A,\theta)e^{i\lambda\Theta}\int_{-\infty}^{o} e^{-i\lambda(a_F\tau-\bar\theta_{Fn})} r_A d\xi$$

$$\cdot\frac{4\pi a_F}{r_A}\delta(\tau+x_A-\xi_F)\delta(\theta_{0F}+\varphi_{0A}+2\Theta+\bar\theta_{Fn}-a_F\tau)\,d\tau$$

$$= \int_\xi \sum_{\lambda=0} \Delta p_F^{(\lambda)}(\xi_F, r_A,\theta)e^{i\lambda\Theta}e^{i\lambda\left[a_F(x_A-\xi_F)+\bar\theta_{Fn}\right]} r_A\frac{4\pi a_F}{r_A}$$

$$\delta\left[\theta_{0F}+\varphi_{0A}+2\Theta+\bar\theta_{Fn}+a_F(x_A-\xi_F)\right]d\xi$$

$$\theta_{0F} = a_F\xi_F = \sigma_F^r - \theta_{bF}^r\cos\theta_\alpha$$

$$a_F d\xi_F = \theta_{bF}^r \sin\theta_\alpha d\theta_\alpha$$

$$\varphi_{0A} = a_A x - \epsilon a_A \qquad x_A = \frac{\varphi_{0A}}{a_A} + \epsilon$$

$$L_F = \Delta p_F \cdot r\theta_{bF}^r$$

$$\{\} = 4\pi\int_o^\pi \sum_{\lambda=0} L_F^{(\lambda)}(r_A,\theta_\alpha)e^{i\lambda\Theta}e^{i\lambda\left(\frac{a_F}{a_A}\varphi_{0A}+a_F\epsilon-\theta_{0F}+\bar\theta_{Fn}\right)}\frac{1}{r_A}\delta\left[\left(1+\frac{a_F}{a_A}\right)\varphi_{0A}\right.$$

$$\left.+a_F\epsilon+\bar\theta_{Fn}+2\Theta\right]\sin\theta_\alpha d\theta_\alpha$$

The induction can be expressed as

$$\Delta W_A^{(1)} = \sum_{n=-\infty}^{\infty} C_n e^{in\Theta} \qquad C_n = \frac{1}{2\pi}\int_{-\pi}^{\pi} \Delta W_A\, e^{-in\Theta} d\Theta$$

Let $\Theta = \theta'$

$$\{\ \} = \sum_{n=-\infty}^{\infty} 2e^{in\theta'} \int_{\theta_\alpha=0}^{\pi} \int_{\theta'=-\pi}^{\pi} \sum_{\lambda} L_F^{(\lambda)}(r_A,\theta_\alpha) e^{i(\lambda-n)\theta'} e^{i\lambda\left(\frac{a_F}{a_A}\varphi_{0A}+a_F\epsilon-\theta_{0F}+\bar{\theta}_{Fn}\right)}$$

$$\frac{1}{r_A}\,\delta\left[\left(1+\frac{a_F}{a_A}\right)\varphi_{0A}+a_F\epsilon+\bar{\theta}_{Fn}+2\theta'\right]\sin\theta_\alpha d\theta_\alpha d\theta'$$

or

$$\{\ \} = \sum_{n=-\infty}^{\infty} 2e^{in\theta'} \int_{o}^{\pi} \sum_{\lambda} L_F^{(\lambda)}(r_A,\theta_\alpha)\, e^{i\lambda\left[\frac{-a_F\epsilon}{2}+\frac{\bar{\theta}_{Fn}}{2}-\theta_{0F}-\frac{1}{2}\left(1-\frac{a_F}{a_A}\varphi_{0A}\right)\right]}$$

$$\cdot\, e^{in\left[\frac{-a_F\epsilon}{2}+\frac{\bar{\theta}_{Fn}}{2}+\frac{1}{2}\left(1+\frac{a_F}{a_A}\right)\varphi_{0A}\right]} \frac{1}{r_A}\sin\theta_\alpha d\theta_\alpha$$

$$= \sum_{n=-\infty}^{\infty} \frac{2e^{in\theta'}}{r_A} \int_{o}^{\pi} \sum_{\lambda} L_F^{(\lambda)}(r_A,\theta_\alpha) e^{\frac{i(\lambda+n)}{2}(a_F\epsilon+\bar{\theta}_{Fn})} e^{\frac{i(\lambda+n)}{2}\frac{a_F}{a_A}\varphi_{0A}}$$

$$\cdot\, e^{-i\lambda\theta_{0F}}\, e^{-i\left(\frac{\lambda-n}{2}\right)\varphi_{0A}} \sin\theta_\alpha d\theta_\alpha$$

Since $\sum_{n=1}^{N_F} e^{\frac{i(\lambda+n)}{2}\bar{\theta}_{Fn}} = \begin{cases} N_F & \text{when } \lambda+n = 2\ell N_F,\ \ell=0,\pm1,\pm2,\ \ldots \\ 0 & \text{otherwise} \end{cases}$

Equation (A-4) becomes

$$\Delta W_A^{(1)} = -\frac{N_F}{2\pi\rho_f U} \frac{1}{\sqrt{1+a_A^2 r_A^2}} \left(a_A r_A - \frac{1}{a_A r_A}\right) \frac{1}{r_A} \sum_{n=-\infty}^{\infty} e^{in\theta}$$

$$\cdot \int_{o}^{\pi} \sum_{\lambda} L_F^{(\lambda)}(r_A,\theta_\alpha) e^{i\ell N_F a_F\epsilon}\, e^{-i\lambda\theta_{0F}}\, e^{-i\lambda\varphi_{0A}}\, e^{i\ell N_F\left(1+\frac{a_F}{a_A}\right)\varphi_{0A}}$$

$$\cdot \sin\theta_\alpha d\theta_\alpha \qquad \text{(A-5)}$$

Assuming

$$L_F^{(\lambda)}(r_A,\theta_\alpha) = \frac{1}{\pi}\sum_{\bar{n}=1} L_F^{(\lambda,\bar{n})}(r_A)\,\Theta(\bar{n})$$

where $\Theta(\bar{n})$ represents the Birnbaum chordwise modes, then the integral part of (A-5) becomes

$$I_{\theta_\alpha} = \sum_{\bar{n}=1}^{\max \bar{n}} \sum_{\lambda=0} L_F^{(\lambda,\bar{n})}(r_A)\, e^{i\ell N_F a_F \epsilon}\, e^{-i\lambda(\sigma_F+\sigma_A)}\, \Lambda^{(\bar{n})}(-\lambda\theta_{bF})$$

$$\cdot\, e^{i\ell N_F\left(1+\frac{a_F}{a_A}\right)\sigma_A}\, e^{-i\left[\ell N_F\left(1+\frac{a_F}{a_A}\right)-\lambda\right]\theta_{bA}\cos\varphi_\alpha} \qquad (A\text{-}6)$$

Taking the lift operator at each $\bar{m}$ and nondimensionalizing with respect to r_{F0}, Eq.(A-5) can be expressed as

$$\left(\frac{\Delta W_A^{(n,\bar{m})}}{U}\right)_I = -\frac{N_F}{2\pi\rho_f U^2 r_{F0}}\left(\frac{1}{\sqrt{1+a_A^2 r_A^2}}\right)\left(a_A r_A - \frac{1}{a_A r_A}\right)\frac{1}{r_A}$$

$$\cdot \sum_{n=-\infty}^{\infty} e^{in\Theta}\, e^{in\left(\frac{a_F\epsilon}{2}+\sigma_A\right)}\, e^{i\ell N_F\left(\frac{a_F}{a_A}-1\right)\sigma_A} \sum_{\bar{n}=1}\sum_{\lambda=0} L_F^{(\lambda,\bar{n})}(r_A)$$

$$\cdot\, e^{-i\lambda\left(\sigma_F-\frac{a_F\epsilon}{2}\right)}\, \Lambda^{(\bar{n})}(-\lambda\theta_{bF})\, I^{(\bar{m})}\left[\left(-n+\ell N_F\left(1-\frac{a_F}{a_A}\right)\right)\theta_{bA}\right] \qquad (A\text{-}7)$$

It can be shown by a similar approach that the second term on the right-hand side of Eq.(A-3) does not contribute to $\frac{\partial^2}{\partial x_A^2}\left(\frac{1}{R}\right)$. Therefore Eq.(A-7) is the only contribution in forming the additional wake effect $\frac{\Delta W_A}{U}$ because the after propeller operates in the race of the forward propeller.

APPENDIX B

THE VISCOUS WAKES OF COUNTERROTATING PROPELLERS

In a counterrotating propulsive system the after propeller, being located in the wake of the forward propeller, operates in a real fluid and hence should include both the potential and viscous effects. In the absence of wake measurements in the plane of the after propeller when the forward propeller is in place, it is necessary to devise a method which will take cognizance of the fact that the after propeller operates in a wake in which the potential and viscous effects should be taken into account. The potential contribution has already been dealt with in Appendix A. The effect of the viscous wake is approximately considered by the Kemp-Sears method described in Reference 16.*

The configuration of viscous wakes of propeller blades is approximated from single airfoil experiments. The unsteady force-and-moment on a downstream blade passing through such wakes is then calculated on the basis of the theory of isolated thin airfoil in nonuniform flow. The same approach has been adapted to the unsteady lifting surface theory. (See Figure 3.)

Silverstein, Katzoff, and Bullivant[17] have shown that the half-width of the wake, Y , may be calculated from the following formula

$$Y = 0.68\sqrt{2}\ C_D^{\frac{1}{2}}\ c(x/c - 0.7)^{\frac{1}{2}} \qquad \text{(B-1)}$$

where

c = airfoil half-chord

x = distance measured along the wake axis (free-stream direction) rearward from the center of the airfoil

C_D = the airfoil profile-drag coefficient

Note: C_D will be calculated according to Hoerner's method.[20]

For convenience, a new coordinate x^* along the wake axis is introduced in Eq.(B-1):

$$x^* \equiv x - 0.7c \qquad \text{(B-2)}$$

Kemp and Sears[16] have shown that in terms of x^* the wake half-width and

*Suggested by Dr. J.P. Breslin.

the velocity at the center become

$$Y = 0.68\sqrt{2}\, c(C_D x^*/c)^{\frac{1}{2}} \tag{B-3}$$

$$u_c/V = -(2.42 C_D^{\frac{1}{2}})/(x^*/c + 0.3) \tag{B-4}$$

and that the velocity profile to be used is

$$\frac{u}{u_c} = \exp\left[-\pi\left(\frac{y}{Y}\right)^2\right] \tag{B-5}$$

Since the propeller blade moves along a line oblique to the x (or x^*) axis, it is convenient to introduce oblique coordinates x',y' as shown in Figure 3. The relation between x^*, y and x',y' is given by

$$x^* = x' - y'\cos\theta_p^F \quad , \quad y = y'\sin\theta_p^F \tag{B-6}$$

where the superscripts F and A refer to the forward and after propeller blades, respectively.

Since the wake is narrow in the region of interest, see Figure 3, y'/x' is small in the wake itself, and one may write, approximately,

$$x^* \approx x' \quad , \quad y \approx y'\sin\theta_p^F \tag{B-7}$$

Then the wake half-width and centerline velocity are as follows:

$$\frac{Y}{r_o} = 0.68\left[C_D^F\left(\frac{x^*}{r_o}\right)\left(\frac{c^F}{r_o}\right)\right]^{\frac{1}{2}} \tag{B-8}$$

$$\frac{u_c}{V^F} = -\left(2.42\sqrt{C_D^F}\right)\Big/\left(\frac{x'}{c^F} + 0.3\right) \tag{B-9}$$

where c^F is the total chord length of the forward propeller.

The velocity profile from Eq.(B-5) is now

$$\frac{u}{u_c} = \exp\left[-\pi\left(\frac{\sin\theta_p^F}{Y}\right)^2 y'^2\right] \tag{B-10}$$

and

$$y' = S(\theta - \frac{\omega\epsilon}{U} - \gamma)$$

$$\therefore \quad \frac{u}{u_c} = \exp\left[-\pi\left(\frac{S \sin\theta_p^F}{\gamma}\right)^2 \left(\theta - \frac{\omega\epsilon}{U} - \gamma\right)^2\right] \tag{B-11}$$

where

θ — angular coordinate of the forward propeller

γ — angular coordinate of the aft propeller

S — radial position (see Fig. 3)

Equation (B-11) can be expanded in a Fourier series in terms of $(\theta-\gamma)$

$$\frac{u}{u_c} = \sum_n \left(a_n \cos n(\theta-\gamma) + b_n \sin n(\theta-\gamma)\right) \tag{B-12}$$

or

$$\frac{u}{u_c} = \sum_n (a_n \cos n\varphi + b_n \sin n\varphi) \tag{B-13}$$

where

$$\varphi = \theta - \gamma \tag{B-14}$$

$$a_n = \frac{N^A}{2\pi} \int_0^{2\pi} \left(\frac{u}{u_c}\right) \cos n\varphi \, d\varphi \quad (N^A = \text{no. of blades of aft propeller}) \tag{B-15}$$

$$b_n = \frac{N^A}{2\pi} \int_0^{2\pi} \left(\frac{u}{u_c}\right) \sin n\varphi \, d\varphi \tag{B-16}$$

The velocity, u_c, is in the direction of x^*, which makes an angle $(\theta_p^F+\theta_p^A)$ with the after propeller blade so that the component giving upwash at the blade is

$$\frac{u_c^n}{U} = \frac{u_c}{V^F} \cdot \frac{V^F}{U} \sin(\theta_p^F+\theta_p^A) \tag{B-17}$$

and since

$$\frac{V^F}{U} \approx \frac{1}{\sin\theta_p^F}$$

then from Eqs.(B-9) and (B-17), we have

$$\frac{u_c^n}{U} = -\frac{\left(2.42\sqrt{C_D^F}\right)}{\left(\frac{x'}{c^F} + 0.3\right)} \cdot \frac{1}{\sin\theta_p^F} \sin\left(\theta_p^A + \theta_p^F\right) \tag{B-18}$$

where

$$\frac{x'}{c^F} = \frac{c^A}{c^F}\left(\frac{\varepsilon}{c^A} \csc \theta_p^F + \frac{x^A}{c^A} \cdot \frac{V^F}{V^A}\right) - 0.7 \tag{B-19}$$

Choose $\frac{x^A}{c^A} = 0$, which means the point is at the mid-chord of the aft propeller blade. Then

$$\frac{x'}{c^F} = \frac{\frac{\varepsilon}{\gamma_o}}{\left(\frac{c^F}{\gamma_o}\right)} \csc \theta_p^F - 0.7 \tag{B-20}$$

The viscous wake, then, can be expressed in the following form:

$$\frac{u^{(q)}}{U} = \frac{u_c^n}{U}\left(a_n \cos n\varphi + b_n \sin n\varphi\right) \tag{B-21}$$

where

$$q = 2n \tag{B-22}$$

$$\varphi = \theta - \gamma = 2\theta \tag{B-23}$$

The left-hand side due to unsteady wake in the PPEXACT (Propeller-propeller Exact) program (Reference 9) is, in lift operator form,

$$\frac{\tilde{w}^{(q,\bar{m})}}{U}(r) = \frac{u^{(q)}}{U}(r)\, e^{-iq\sigma^r}\, I^{(\bar{m})}\left(q\theta_b^r\right) \tag{B-24}$$

where

$$I^{(\bar{m})}\left(q\theta_b^r\right) = \frac{1}{\pi}\int_0^{\pi} \Phi(\bar{m})\, e^{iq\theta_b^r \cos\varphi_\alpha}\, d\varphi_\alpha \tag{B-25}$$

$$\Phi(1) = 1 - \cos\varphi_\alpha$$

$$\Phi(2) = 1 + 2\cos\varphi_\alpha$$

$$\Phi(\bar{m}) = \cos(\bar{m}-1)\varphi_\alpha \qquad \text{for } \bar{m} > 2$$

Thus, the resulting unsteady force and moment or unsteady side force and moment, at the specified blade frequency, can be determined as in the PPEXACT program. These viscous effects are then superposed on the results from the potential flow of the CRP system.

DISTRIBUTION LIST
(Contract N00014-77-C-0298)

15 Commander
DAVID W. TAYLOR NAVAL SHIP R&D CENTER
Bethesda, MD 20084

Attn: Code 1505, Bldg 19, Room 129B

9 Commander
NAVAL SEA SYSTEMS COMMAND
Washington, DC 20362

Attn: 03R22 (J. Sejd)
312 (C. Kennel)
3213 (R. Keane, Jr.)
05H (A. Paladino)
321X (S. Cauldwell)
52
521 (F. Welling)
524 (P. Petros)
99612 (Library)

12 Director
DEFENSE TECHNICAL INFORMATION CENTER
5010 Duke Street
Alexandria, VA 22314

1 Dr. Robert E. Whitehead
Code 432
OFFICE OF NAVAL RESEARCH
800 N. Quincy Street
Arlington, VA 22217

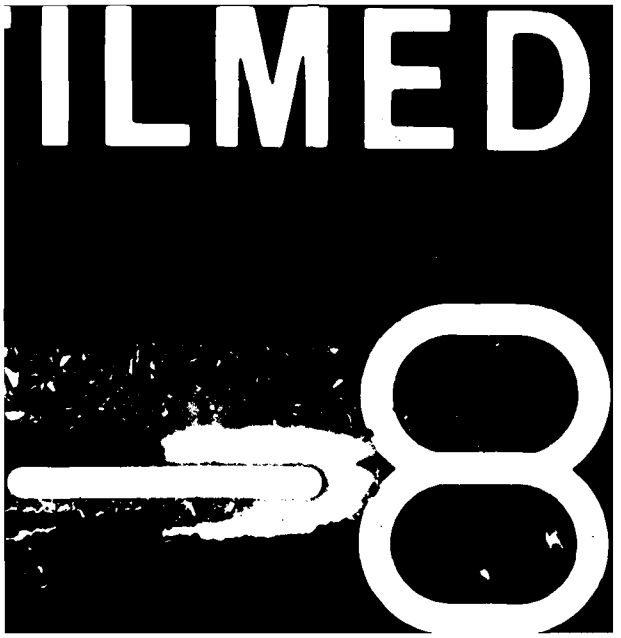
ILMED
8